A NUMERICAL STUDY ON LONG-TERM GROUND DEFORMATION DURING TUNNELING THROUGH CLAY

Thesis submitted in partial fulfillment of the requirement for the degree of
Master of Civil Engineering
In

Soil Mechanics and Foundation Engineering

By

Subhadeep Das

Roll No.: 002110402021

Examination Roll No.: **M4CIV23019B**

Registration No. **160036** of **2021-2022**

Under the guidance of

Prof. Ramendu Bikas Sahu

Professor
Department of Civil Engineering
Jadavpur University
Kolkata – 700032

Department of Civil Engineering
Faculty of Engineering & Technology
Jadavpur University
Kolkata – 700032

2023

DECLARATION OF ORIGINALITY AND COMPLIANCE OF ACADEMIC ETHICS

This is to declare that I, **Subhadeep Das**, student of Geotechnical Engineering Division of the Department of Civil Engineering, class roll no. **002110402021**, have prepared this thesis entitled "**A NUMERICAL STUDY ON LONG-TERM GROUND DEFORMATION DURING TUNNELING THROUGH CLAY**" under the supervision of Prof. Ramendu Bikas Sahu. This manuscript is original and not directly plagiarized in any sense. However, the Literature studied for the preparation of this report has been cited wherever required and also presented in the list of references.

Date:

Subhadeep Das
Roll No.: 002110402021
Department of Civil Engineering
Jadavpur University, Kolkata

CERTIFICATE

This is to certify that the thesis entitled — **"A NUMERICAL STUDY ON LONG-TERM GROUND DEFORMATION DURING TUNNELING THROUGH CLAY"** has been carried out by **Subhadeep Das** bearing Class Roll No: **002110402021**, Examination Roll No.: **M4CIV23019B** and Registration No: **160036 of 2021-2022**, under my guidance and supervision and be accepted in partial fulfillment of the requirement for the degree of Master of Engineering in Soil Mechanics and Foundation Engineering in the Department of Civil Engineering.

Prof. Ramendu Bikas Sahu
Professor
Department of Civil Engineering
Jadavpur University
Kolkata - 700032

Head of the Department
Department of Civil Engineering
Jadavpur University
Kolkata – 700032

Dean
Faculty of Engineering and
Technology
Jadavpur University
Kolkata – 700032

FACULTY OF ENGINEERING & TECHNOLOGY

JADAVPUR UNIVERSITY

CERTIFICATE OF APPROVAL

The forgoing thesis titled **"A NUMERICAL STUDY ON LONG-TERM GROUND DEFORMATION DURING TUNNELING THROUGH CLAY"** is hereby approved as a creditworthy study of an engineering subject conducted and presented satisfactorily to warrant its acceptance as a precondition to the degree for which it was submitted. It is understood that the undersigned does not automatically support or accept any argument made, opinion expressed, or inference drawn in it by this approval, but only approves the thesis for the reason it was submitted.

Committee on Final Examination

for Evaluation of the Thesis

_____

Signature of External Examiner

_____

Signature of Supervisor

ACKNOWLEDGEMENT

I, Subhadeep Das, bearing Roll No. 002110402021 would like to take this opportunity to thank my supervisor, Prof. Ramendu Bikas Sahu, for his constant guidance and support without which this work wouldn't have been possible. I would also like to thank Prof. Sibapriya Mukherjee (Retd.), Prof. Gupinath Bhandari, Prof. Sumit Kr. Biswas, Prof. Narayan Roy, Dr. Arghadeep Biswas and Dr. Obaidur Rahaman, who have imparted their valuable knowledge throughout the course.

I would be failing in my duties if I didn't thank my classmates, especially Ajfar and Shubhadip. Constant discussion with them uplifted the quality of this work significantly.

For Maa and Baba, who have consistently been my source of unwavering support, expressing sufficient gratitude would always fall short.

Date:

Place: Jadavpur

Subhadeep Das

Soil Mechanics and Foundation Engineering

Department of Civil Engineering

Jadavpur University

Kolkata-32, West Bengal, India

ABSTRACT

Increasingly complex transportation infrastructure, limited land, and the need for more efficient underground space use have led to a rising demand for tunnels. Tunnels offer versatile solutions, addressing barriers, environmental concerns, cultural preservation, and urban hygiene. However, tunnel design in geotechnical engineering is complex, influenced by factors like subsoil properties, groundwater, and potential risks in challenging conditions like high groundwater tables or soft clay, which can result in unforeseen accidents.

This research delves into the response of clay to tunnel excavation and the consequential long-term ground deformations, a critical aspect for ensuring safety. To investigate this, PLAXIS 3D's Finite Element analysis (FEA) will be utilized. Stress variations at various depths, as well as their associated stress paths, will be graphed, and an effort will be made to identify the potential correlations. Furthermore, an in-depth examination will be conducted on the volume of lost ground and its impact on tunnel stability.

TABLE OF CONTENTS

LIST OF FIGURES

LIST OF TABLES

Chapter 1 : **INTRODUCTION**

1.1 GENERAL BACKGROUND

Some 3000 years ago, when our ancestors started discovering techniques of building stable and strong bridges, they also discovered new ways of connecting two points of land - tunnels! This discovery was initially used not for transport of goods and people across harsh terrains, but for defensive purposes in the vicinities of important military or royal posts (tunnels below castles). Babylonian and Persian architects were the first who saw the potential of large underground networks of tunnels called quant or kareez. These irrigation tunnels were used to transport water underground through deserts, enabling life in some of the most hostile lands on planet earth. Iranian city of Gonabad still has a working network of kareez tunnels that is 2700-year-old. In Babylonia, royal families enjoyed fresh water from Euphrates that was delivered to them through incredibly built 900m long tunnel that was lined with bricks.

Greeks and roman took all the knowledge of Babylon and Ancient Egypt, and improved it ten-fold. With tunnels they were able to transforms marches, transport water through mountains, and create pedestrian tunnels trough very harsh terrains. To this day historians wonder how much workforce was involved in the construction tunnel between Naples and Pozzuoli that was created around 36 B.C. This incredible structure was 4800 foot long, 25 foot wide and 30 foot high, and it even had ventilation shafts. Less than 100 years later in 41 A.D., Romans used around 30,000 workers to build even larger tunnel that was 5.6 km long. After 11 years of work, tunnel finally enabled drainage of the Fucine Lake, which shrunk from its original size of 140 km^2 to 57 km^2. Later in 19th century, Italian prince Alessandro Torlonia commissioned complete drainage of that lake, which was done by the efforts of the Swiss engineer Franz Mayor de Montricher who created new tunnel after 13 years of work. Land that was reclaimed from that lake represents one of the most fertile stretches of land in the entire Italy.

In European Middle Ages, tunnels were almost exclusively used for mining or for military. After public transportation finally started to grow under the influence of Renaissance and trading with distant lands. Hundreds of smaller tunnels were created between mid-1600s and 19th century, but by then new driving force of tunnel construction came – railroads. This new form of transport soon enabled spreading of tunnels across entire world.

Tunnels, as defined by the American Association of State Highway and Transportation Officials (AASHTO) Technical Committee for Tunnels (T-20), are enclosed roadways with vehicle access that is restricted to portals regardless of type of the structure or method of construction. It is also further defined that tunnels not to include enclosed roadway created by highway bridges, railroad bridges or other bridges.

1.2 GENESIS OF THE PROBLEM

The increased use of underground space for transportation systems and the increasing complexity and constraints of constructing and maintaining above ground transportation infrastructure have prompted the need to the use of tunnels. Also, open unused lands are hard to go by nowadays. Hence the spaces required for construction of above ground transportation facilities are also in scarcity. Even this reason spurred us to venture into the third dimension - depth.

Tunnels are feasible alternatives to cross a water body or traverse through physical barriers such as mountains, existing roadways, railroads, or facilities; or to satisfy environmental or ecological requirements. In addition, tunnels are viable means to minimize potential environmental impact such as traffic congestion, pedestrian movement, air quality, noise pollution, or visual intrusion; to protect areas of special cultural or historical value such as conservation of districts, buildings or private properties; or for other sustainability reasons such as to avoid the impact on natural habit or reduce disturbance to surface land. They also cause least disturbances during installation and maintenance.

Tunnels also play a major role in maintaining the overall hygiene of a city, by helping convey clean water to houses and waste water from houses and industries to treatment plants. In a line, it can be said that, tunnels help in the environmental, ecological, economic and social well-being.

1.3 PROBLEM DEFINITION

The nature and engineering behavior of the ground to be tunneled through are fundamental considerations in the design of tunnel. This becomes elemental when the tunnel goes through soft soil or a cluster of boulders. There comes several parameters, the subsoil properties and the properties of the tunnel, from effect of the ground water table and methodology of analysis to the construction sequence. The presence of alluvial soil with ground water table becomes extremely challenging for the tunnel designer. Moreover, if the subsoil consists of soft clay, to get the tunnel through it, severe accidents may happen due to unforeseen circumstances, as in

the case of Bowbazar, Kolkata, causing massive property damage and delay of the project, eventually risking dissipation of pressure and further deteriorating the situation in another way.

Hence, tunnel stability analysis becomes a point of utmost importance and should be given care to. A tunnel construction is always accompanied with an amount of volume loss of the ground. And this lost volume determines whether or not the tunnel is stable. There have been many such catastrophe which has occurred as tunnel safety and ground deformation haven't been catered to. Fig. 1.1 & 1.2 shows some of such tunnel failures in the recent history.

Figure 1.1 (a) Failure of an under-construction tunnel in Ramban district, J&K, May 2022 **(b)** Rastatt tunnel collapse, Germany, considered as of the most classic examples of tunnel failure. It consisted of twin track railway corridor between Germany and Switzerland. It was being constructed with the support of horizontal ground freezing through water-bearing sands and gravels. But failed with failure of the ground freezing regime and loss of integrity of the segmental lining, allowing ground loss under the rail tracks into the new tunnel bore beneath.

Figure 1.2 (a) Underground tunnel collapse causing a sinkhole in Kuala Lumpur, July 2014 **(b)** Sao Paulo tunnel failure due to "systemic failure" of design, construction and risk management, January 2007.

1.4 CASE STUDIES

Table 1.1 Case studies of some significant tunnel construction in India

Sl. No.	Tunnel and its location	Specifications	Constructed by	Method of construct-ion	Purpose	Challenges Faced
1	**East-West Metro tunnel, Kolkata**	Length-10.8km Width-5.5m With a 520m stretch going beneath the Hooghly River and average roof-to-ground distance of 30m	Kolkata Metro Rail Corp.	Tunnel Boring Machine (TBM)	Metro tunnel connecting Phoolbag-an and Howrah Maidan metro stations	Being the first underwater tunnel in India, it had its complications. In 2019, a TBM hit an aquifer which led to collapse of structures.
2	**North-South Metro tunnel, Kolkata**	Length-16.5km With broad gauge track, having 15 underground and 2 at-ground stations	Metropolitan Transport Project (Railways)	Cut-and-cover method and Driven shield tunneling	Metro tunnel connecting Dumdum and Tollygunge metro stations (N-S corridors)	Being India's first metro tunnel, it was more of a trial-and-error affair. Two different methods had to be adopted to maintain the alignment.
3	**Atal Road tunnel, HP**	Length-9.02km Width-10m With two lanes at an elevation of 3100m Horse-shoe in shape	Border Road Organization (BRO)	Drill-and-blast coupled with new Austrian Tunneling method	Highway tunnel that reduces the travel time and overall distance between Manali and Keylong on the way to Leh	Freezing temperature, difficult weather conditions and avalanche spots made excavation difficult, reducing its rate. Most of the excavation was done from the southern part.

4	**Pir Panjal Railway tunnel, J&K**	Length-11.6km Width-8.4m Height-7.39m at an average altitude of 1760m	Hindustan Construction Company	New Austrian Tunneling method (NATM)	To increase connectivity to J&K, this rail tunnel was built. As the already existing Jawahar tunnel (road) was inoperable in winters.	Change in geological conditions and the different nature of rocks, hindered the work. Soft clay and existence of villages over tunnel alignment made excavation difficult. Heavy ingress of water and seismic zones had to be kept in mind.
5	**Dr. Syama Prasad Mookherjee Road tunnel, J&K**	Length-9.03km Width-13m with two lanes, at an average altitude of 1200m	IL&FS Transportation Networks (ITNL)	New Austrian Tunneling method (NATM)	India's longest road tunnel, reduces the distance between Jammu and Srinagar by 30 km and travel time by two hours	The topography as well as the seismic nature of the area, posed various challenges in the design.
6	**Trivandrum Port Railway tunnel, Kerala**	Length-9.02km is going to be the second longest railway tunnel in	Konkan Railway Corp.	New Austrian Tunneling method (NATM)	A 10.7-km railway line, including a 9.02-km	Land acquisition from the nearby villages, seemed to be a potential

		India on completion			tunnel, has been proposed to connect the upcoming Vizhinjam International Multipurpose Deepwater Seaport to the railway network	hurdle in the project.

1.5 OBJECTIVE & SCOPE OF WORK

1.5.1 *Objective*

This study aims to investigate how soft clay responds to tunnel excavation and the subsequent long-term ground deformations. Given its low shear strength, understanding these deformations is vital for safety. We'll use Finite Element analysis in PLAXIS 3D to achieve this, along with examining stress changes with depth, stress paths, and other relevant factors.

1.5.2 *Scope of work*

- Numerical analysis to be done by PLAXIS 3D. Finite element analysis will be done to model the tunnel and evaluate the different parameters using numerical methods.
- Ground deformations during tunneling in soft clay are also being studied. Different profiles thus obtained are going to be analyzed and interpreted.
- Also, further studies are conducted to get to a conclusion about the deformed patterns.
- A separate study on volume loss is also being done in the current thesis.

1.6 ORGANIZATION OF THE THESIS WORK

The thesis will be broken down into several chapters for an easier breakdown of the work. Initially, the work plan for the 5 chapters is finalized as described below.

Chapter 1 serves as an introduction to the entire thesis.

Chapter 2 showcases a collection of studies related to tunnels. The chapter concludes by providing a summary of the reviewed literature and offering an in-depth explanation of the current study's scope.

Chapter 3 focuses on the materials and research methodology employed in this study. It delves into the specifics of soil parameter utilization, the creation of a geometric model, the selection of model parameters, mesh refinement, and the finite element analysis (FEA) process.

The results obtained from the analysis performed are elaborated in **Chapter 4.** Various analysis to get to the concluding parts, are also being covered in this section.

Chapter 5 presents the summary, conclusions, limitations, and scope of future study. It will also present a brief summary of the present research and conclusions drawn from the obtained results and documents some suggestions on the scope of future study in the related field.

Chapter 2 : **LITERATURE REVIEW**

2.1 INTRODUCTION

In this section, a compilation of past research studies focusing on analyzing ground and tunnel stability when tunneling is being done in different soil, is presented. Studies have been based on many approaches, viz., analytical, numerical and laboratory tests. This in turn has helped engineers and other professionals get a simulation of a critical problem, which was difficult to predict otherwise.

The objective of this particular section within the literature review is to comprehensively assess the advancements achieved in this specific field of study. This involves a meticulous examination and analysis of the existing research findings, with the overarching aim of pinpointing and shedding light on potential avenues for future research.

In essence, this chapter seeks to accomplish a two-fold purpose: firstly, to document and highlight the notable strides that have been made in the field, showcasing the evolution of knowledge, methodologies, and key discoveries over time. This retrospective analysis serves as a foundation upon which to build an understanding of the current state of affairs within the research domain.

Secondly, the critical evaluation undertaken within this section is instrumental in discerning gaps, limitations, or areas where the existing body of research might fall short. By scrutinizing the findings, methodologies, and interpretations of previous studies, it becomes possible to identify promising research opportunities that remain unexplored or require further investigation.

In essence, this chapter acts as a bridge between the past and the future of research in the field, offering a synthesized perspective on the trajectory of knowledge development and serving as a springboard for researchers to embark on new and potentially groundbreaking investigations. It is through this critical analysis and synthesis of past and current research that the intellectual progression of the field is nurtured, fostering a deeper understanding and paving the way for innovative and impactful contributions in the years to come.

2.2 LITERATURE REVIEW

1. **Peck (1969)** focused on past experiences with tunnel-boring machines (TBMs) in Switzerland in his state-of-the-art report where observational data were assembled with respect to the necessary requirements. The author also suggested procedure for design, particularly, in design of tunnel lining, the strength of soil had been taken into account rather than ignoring it completely.

   The author took into account, observations of the lateral movement of sheet piles or soldier piles. The author found that the magnitude of the lateral movement depended on the nature of the soil and the depth of excavation. The lateral movements were significant as they were associated with loss of volume. In cohesionless soil, particular observations were marked for flow of ground, flow of ground water and heave of material at the bottom etc. A Gaussian curve that required two parameters (i.e., maximum settlement at tunnel centre line and distance of the inflection point) was employed to generate the transverse settlement trough.

   The settlement trough was characterized by maximum settlement (δmax), the trough width (i), which was the horizontal distance from the tunnel centre-line to the point where settlement $\delta = 0.61\ \delta max$ and the curvature of the tough changed its direction.

   The settlement then at any distance x is, $\delta = \delta max \exp(-x2/2i2)$ and volume of the settlement trough, $Vs = \sqrt{2\pi}\ i\ \delta max$.

   In this report, the author gave precise apparent pressure diagrams for soft & stiff clayey soil and sands. These are now widely used all over the world. The design procedures of a tunnel in clayey soil, the design of lining the basis of ring stress for design of the tunnel lining, effect of multiple tunnels was all been discussed in detail in this report for easy and comprehensive understanding of the subsoil and tunnel design procedure.

2. A tunnel, even though it is a three-dimensional problem, a two-dimensional idealization would be able to make it more easily analysed, was what had been mentioned by **T. Kimura and R. J. Mair (1983)**. Centrifuge tests were then performed to explore the relationship between the two-dimensional idealization and the more complex three-dimensional tunnel. Soil samples were prepared by consolidating kaolin slurry with undrained shear strength of 26 kPa. Tunnels of 60mm were dug and tested in a 4m

working radius centrifuge under 75g and 125g. Silvered Perspex balls compressed into the clay were then photographed. Then tunnel support (σT/Cu) at the collapse was plotted against cover-to-diameter ratio. The results were seen to be in agreement with the theoretical stability analysis. Failure patterns of the tunnel model under the self-weight of the surrounding soil were also studied in this paper.

3. In his thesis a consistent and comprehensive approach to calculate the settlements above tunnels in soft clay was presented by **Robert Man Ng (1984)**. First, the author presented a simplified approach to predict the maximum settlement and another detailed approach was presented to estimate the pattern of the displacements.

   A gap parameter was used to quantify the loss of volume and to model the soil reconsolidation. The action of tunnel construction produced two physical changes in the soil mass: a) the creation of new boundary within the soil mass, and, b) the removal of the in-situ stresses along the excavated circumference. The loss of ground may be defined as volume of material that had been excavated out in excess of the theoretical volume within the outer diameter of the final tunnel lining. The components of loss of ground may be represented quantitatively by introducing a gap parameter. The gap parameter was a measure of the volume of the ground lost into the tunnel.

   This parameter was calculated from conventional soil parameters and it validated reasonably with actual field data. This parameter was then used to determine the ground settlement from an empirical relationship derived from fifteen case studies. However, appropriate consideration of the stress path was necessary to determine the design soil parameters.

   The author diligently identified the Thunder Bay tunnel area subsoil system several field and laboratory tests had been conducted and the results were used to discriminate the subsoil properties. Specific focus had been made by the author on the tunnel instruments as well as the construction sequence to arrive quantify the effect of these qualitative factors on the gap factor, and consequently the stability of the tunnel & settlement of the surface above it.

4. Until then, the principal method of designing the stability of a tunnel was done as per empirical method suggested by Peck (1969). **Loganathan & Poulos (1998)** analyzed that for a ground deformation prediction due to tunneling to be accurate, the prediction method should account for the effect of a number of parameters, such as tunnel construction method and tunnel-driving details, tunnel depth and diameter, initial stress state, and stress strain behavior of the soil around tunnel. The definition of the traditional ground loss parameter was redefined with respect to the gap parameter and incorporated into the closed form solution derived by Verruijt and Booker (1996).

   The ground loss occured in two stages: (1) Loss in the undrained state, immediately after the passing of the tunnel head; and (2) loss due to time dependent consolidation and creep of the ground. The writers have modified the close form solution by Verruijt and Brooke (1996) to accommodate the newly defined ground loss parameter of the authors that incorporated the nonlinear ground movement around the tunnel soil interface. Since this study was concerned only with short-term undrained conditions, the ground deformations due to long-term localization of the tunnel lining were neglected. The authors also proposed a new method to determine the trough depth which just exceeded the length estimated by other methods such as given by Schmidt (1981) and Mair et al (1981). After that they also proposed a new relationship of lateral deformation.

   Five case studies were done by the authors to estimate and compare the results given by the authors and by other methods, considering Heathow Express Trail Tunnel, U.K., Thunder Bay Tunnel, Canada, Green Park Tunnel, U.K., Barcelona Subway Network Extension, Barcelona and Bangkok Sewer Tunnel, Thailand.

   The applicability of the analytical solutions proposed paper had been evaluated with reference to five case studies. The equivalent ground loss values predicted using the new method are in good agreement with reported empirical ground loss values for tunnels in stiff clay but were overestimated for the case of a tunnel in soft clay. The settlement troughs predicted were slightly wider than those observed or estimated using empirical methods. Good agreement had been observed for sub-surface settlements and horizontal movements for uniform clay profiles.

5. **Wu, B. R. and Lee, C. J. (2003)** performed a series of centrifugal tests of unlined single and parallel tunnels, in plane strain condition. They investigated the ground movement and the collapse mechanism induced by tunneling in soft clay. The surface settlement of a single tunnel was fitted by a normal distribution curve and superposition was done, using modification factors for more than one tunnel. The relationship of the surface and sub-surface settlement troughs was plotted against ground loss with burial depth as a function. And then the results were correlated with established results.

   The ground movements around the tunnels were related to the load (or overload) factor. The increase was seen to be dramatic when the factor was greater than 0.5. The collapse mechanisms obtained for single and parallel tunnels were found to be consistent with the observed field results. The relationship between I and C/D ratio derived from the centrifuge model tests was presented for estimating the width parameter of the surface settlement trough. Maximum settlement could be evaluated from the given relationship. Other relationships between different parameters could also be used for other calculations. The results were further verified against field data, and have been seen to give satisfactory results.

6. **Greenwood (2003)** in his parametric study for MIT evaluated effects of different construction variables on surface settlements for tunneling in soft ground using Plaxis 3D. The author started with different aspects of the construction, using ground parameters, construction methods, stability problems in different parts of the tunnel and then drove through calculation of surface settlement using Attewell and Woodland (1982) method, going further into deriving the settlements through finite element analysis.

   It had been shown through extensive field experience that the best way to contend with the deformation and thus inhibit surface settlement was to pump a pressurized grout into the tail void. The void was continually filled with grout as the machine advances in one of two ways:

   a) Grout was pumped through pre-drilled holes in the pre-cast concrete lining segments; this was the more traditionally used method.

b) Grout was injected through grout ports at the back of the tail skin, i.e., between the inner surface of the tail skin and the outer surface of the lining segments.

In this study, several aspects of the problems were quantified, such as face pressure, jacking force, grout pressure, ground loss and effects of construction stages.

While many methods have been proposed to estimate the transverse settlement trough, the empirical approach suggested by Attewell and Woodman (1982) was the only methodology that attempts to predict longitudinal settlements. Knowledge of the approximate dimensions of the transverse settlement trough allows one to estimate which buildings will be affected by the tunneling process and how much they might settle. While surface structures also tilt inward toward the tunnel centerline when viewed in the transverse cross-section, the tilting in the longitudinal direction happens twice (once as the face approaches the structure and once as it moves back to near its original orientation) compared to the one rotation in the transverse direction. In addition, the evolution of settlement as the shield tunneling advances underneath a given point can be predicted by the method of Attewell and Woodman. This material gives insight into the amount of total settlement, which may be different from the net settlement if the ground ahead of the face is allowed to heave.

In the present analysis, PLAXIS 3D Tunnel was used to conduct a parametric study of the longitudinal settlement profile for a large-diameter tunnel constructed with the EPB method. The chosen problem geometry consists of a tunnel excavated through a normally consolidated clay using the EPB method. The aim of the analysis is to observe the behavior of the settlement trough on the surface as the shield passes through the material while varying the applied pressure at the face and the grout pressure in the tail void.

It was described previously that the plane boundaries (z-planes) are fixed so that no displacement is allowed in the z-direction, which causes the ground surface to be exactly horizontal at the boundaries. In the case of the front plane boundary, located ahead of the tunnel face, this boundary effect introduces some inaccuracies in the amount of heave/settlement, especially in the later construction phases as the face approached the front plane boundary. In essence, the higher the face pressure (i.e., the lower the overload factor), the greater the increase in the amount of ground heave ahead of the tunnel face due to the boundary effect.

At the rear plane boundary, located behind the advancing shield, a similar problem was encountered, even in the later construction phases when the boundary is farthest from the advancing face. The boundary effect influences the longitudinal settlement profile above the lining for cases in which the applied face pressure is high or low (N 3 and above and N= 0 and below).

Maximum surface settlement is not always the most important factor in minimizing damage to buildings on the surface. The total settlement, as defined above, is important because a building may heave and then undergo an amount of settlement greater than the difference between its final and initial positions. This additional movement may cause further damage to a structure than the maximum surface settlement might suggest. This study confirms Peck's (1969) work of the soil body should not have failed inward through the face at an overload factor of 4.5.

It is found in this study that the amount of heave ahead of the tunnel face increases with increasing face pressure and the amount of vertical settlement above the lining decreases with increasing face pressure up to a point, after which it increases slightly. Also, as expected, the amount of vertical settlement above the lining decreases with increasing grout pressure.

7. Physical modeling has played a crucial role in the examination of tunnel excavation in soft ground, with researchers globally developing a range of techniques to investigate how the ground responds to tunneling. These methods span from two-dimensional trap door tests to the use of miniature tunnel boring machines within a centrifuge, emulating the tunnel excavation and lining installation process. In their paper, **M.A. Meguid et al. (2007)** provided an overview of specific physical models used in soft ground tunneling research. Furthermore, the paper delved into the various approaches employed for recording soil deformation and failure mechanisms resulting from tunneling, presenting experimental setups and sample results for each technique as originally described by the authors. The paper also included a summary of the pros and cons associated with each method.

   Physical modeling of tunnels in soft ground being an integral part of tunnel analysis and design, over the years, researchers worldwide have developed and implemented diverse techniques to simulate tunnel excavation processes. While reduced-scale tests

conducted under 1g conditions allowed precise control over the excavation process, they did not accurately replicate in-situ stress conditions. Centrifuge testing, on the other hand, enabled a more realistic simulation of in-situ stresses, but it required simplifying the tunnel construction process. Various methods have been devised to emulate tunnel construction in soft ground, such as the trap door method, which successfully simulated soil arching around excavated tunnels. This method permitted the investigation of vertical stresses and surface displacements under 2D or 3D conditions. Tunnel face stability was assessable using a rigid tube with a flexible membrane at the face, where tunnel excavation was simulated by reducing air pressure within the tunnel and monitoring soil movements. Other methods, like the dissolvable polystyrene core, achieved some success, although they resulted in non-uniform surface settlement when the excavation occurred underwater. Techniques involving hand or mechanical auguring to represent tunnel excavation and progressive face advance appeared more realistic, but the expense of mechanizing these tests in a centrifuge posed challenges. Consequently, further experimental research was required to enhance existing techniques and develop new methods that could accurately simulate actual tunnel construction.

8. Surface soil settlements resulting from tunneling arise due to stress relief and subsidence caused by the movement of support during excavation. In their **2011** paper, **Mohammed Y. Fattah et al.** explored the shape of settlement depressions induced by tunneling in cohesive ground using various approaches, including analytical solutions, empirical methods, and numerical solutions employing the finite element method. The width of the settlement depression was determined using the finite element method by tracking changes in the slope of the computed settlement profile.

   The findings revealed that the finite element method tended to overestimate the width of the settlement depression when compared to Peck's results for both soft and stiff clay, but it exhibited excellent alignment with Rankine's estimations. The results indicated a strong agreement with the complex variable analysis at z/D = 1.5, while at z/D = 2 and 3, the curve diverged in regions distant from the tunnel's center. Additionally, in an elastic homogeneous medium, the upward soil movement was primarily attributable to

the relief effect of the excavated soil above the tunnel. However, this upward movement decreased as x/D increased.

9. The stability analysis of a tunnel can be done either by analytical approach or empirical methods. However, **Likitlersuang et al., (2014)** in their paper aimed to present simplified methods for ground settlement computation of tunnelling works using the PLAXIS finite-element programme. Three simplified methods – contraction ratio, stress reduction and modified grout pressure – were considered in this study. Practical correlation among these three methods have also been mentioned in this study.

   This paper aimed to present simplified finite-element analyses of tunnelling-induced surface settlement based on the Blue Line Bangkok MRT project. The results were based on a series of finite-element analyses of the Blue Line Bangkok Mass Rapid Transit tunnels. The results of numerical analysis may be influenced by many factors such as simplified geometry and boundary conditions, mesh generation, initial input of ground conditions and constitutive relationships chosen to model the behavior of soils. This paper aimed to present simplified finite-element analyses of tunneling-induced surface settlement based on the Blue Line Bangkok MRT project. A total tunnel length of 20 km (excluding underground stations) was constructed using eight earth pressure balance (EPB) shields (six Kawasaki and two Herrenknecht machines).

   The construction methods used for the tunnelling and the underground stations of the North and South sections had different already fully excavated and with the base slab construction completed. Then, the shield was driven from the north end of sequences. The contractors for the North sections were to start their tunnelling works as soon as possible, with the tunnelling through the eventual station sites to be completed before the station box excavation. In contrast, the EPB shields of the North section commenced work from the Thailand Cultural Centre Station, with a launch shaft located at the north end of the station towards Huai Khwang and Sutthisan Stations, and arrived at the Ratchadaphisek Station, which was fully excavated and with the base slab construction completed. Then, the shield was driven from the north end of Ratchadaphisek Station to Phahon Yothin Station, and involved tunnelling through the incomplete Lad Phrao Station. For the South section, on the other hand, the underground station boxes were excavated and constructed prior to the tunnelling. Hence, the South contractor avoided

the extra length of temporary tunnel, which was approximately equal to the length of the underground station box.

The Bangkok subsoil forms a part of the larger Chao Phraya Plain and consists of a broad basin filled with sedimentary soil deposits. These deposits form alternate layers of sand and clay. Field exploration and laboratory tests from the MRT Blue Line project show that the subsoils, down to a maximum drilling depth of approximately 60–65 m, can be roughly divided into (1) made ground at 0–1 m, (2) soft to medium stiff clays at 1–14 m, (3) stiff to very stiff clays at 14–26 m, (4) first dense sand at 26–37 m, (5) very stiff to hard clays at 37–45 m, (6) second dense sand at 45–52 m and then followed by (7) very stiff to hard clays. The aquifer system beneath the city area is very complex, and the deep well pumping from the aquifers, over the last 50 years, has caused substantial piezometric drawdown in the upper soft and highly compressible clay layer.

The construction sequences for the FEM analysis of tunnelling using TBM can be divided into four major stages: (1) shield advancement and balancing pressure at the face, (2) installation of segmental lining and backfill grouting, (3) grout hardening and (4) hardened grout (Ding et al., 2004; Komiya et al., 1999). While tunnel excavation should be considered ideally as a 3D problem, full 3D numerical analysis is time consuming and requires excessive computational resources. Consequently, simplified 2D analysis could be considered to be sufficiently flexible and economic to find application in practice. Three simplified 2D FEMs named contraction, stress reduction and modified ground methods are employed in this study. Ground responses of the tunnel construction simulation from the three simplified 2D methods are compared in the present study. It is noted that the analyses were carried out based on short-term and uncoupled analysis assumption.

In undertaking the 2D finite-element modelling, a sufficient mesh dimension is required. This process avoids the influence of the finite-element modelling at the boundary of the mesh model. The mesh dimensions adopted in this study follow suggestions of Möller (2006), where the maximum primary stress rotation is limited to less than 2·5° at the bottom boundary. At the left and right boundaries, the maximum vertical strain is kept to a value lower than 1% of the maximum vertical strain at the centreline. The results of his finite-element study with the HSM showed that the distance from the tunnel crown to the bottom boundary (h) should be at least 2·2 times

the tunnel diameter. This criterion is restricted to cases where the tunnel diameter ranged from 4 to 12 m.

The tunnel excavation techniques involve 3D phenomena. Simulating tunnel excavation in the 2D plane-strain finite-element analysis requires a number of assumptions to govern the missing dimension. In this study, the grout pressure method was modified. This modified method used three calculation phases. Three methods (contraction method, stress reduction method and modified grout method) were used to model tunneling in the 2D finite-element analysis. It is seen that all three methods provided a sensible degree of matching for the predicted surface settlement profiles. They were also very similar in shape to the surface settlement profiles. All the clay layers (Bangkok soft clay, first and second stiff clay, and hard clay) within the selected soil profiles were modeled as undrained.

All seven sections of the Bangkok MRT twin tunnels were modeled using three 2D simplified methods and presented in this study. The data from the actual measurement and back analysis data are compared and the relationship between contraction, stress reduction and modified grout pressure methods has been identified. The calculated percentage of contraction from the finite element analysis and the calculated percentage of the volume loss from the Gaussian curve and the superposition technique were found comparable. Simplified 2D finite-element modelling can be used reasonably to solve the 3D problems of tunnelling-induced ground surface settlements.

10. In their **2015** paper, **Soranzo, E. et al.** conducted an investigation into the stability of tunnel faces in shallow tunnels situated within partially saturated soil using a combination of centrifuge testing and numerical analysis. They selected loess soil as the focus of their study and characterized its properties through laboratory testing. Centrifuge model experiments were conducted under varying soil densities and water table depths, while numerical analyses were carried out using an advanced constitutive model designed for partially saturated soil. This constitutive model was incorporated into a finite-element software utilizing Bishop's effective stress principle, and its parameters were fine-tuned based on drained triaxial compression tests conducted on partially saturated soil. To simulate the collapse of the tunnel face due to wetting, a

zero-pore pressure condition was imposed at the ground surface, and the numerical results were subsequently compared with the outcomes of the centrifuge tests.

In the context of shallow tunnels, ensuring the stability of the tunnel face was of paramount importance to prevent excessive ground movement and tunnel failure. When the tunnel was either fully or partially submerged below the groundwater level, dewatering was often carried out during the construction phase.

While the benefits of dewatering in tunneling were well-known within the industry (Pujades et al., 2014), a comprehensive model for quantitatively assessing its effects had been lacking. The authors of this study introduced a numerical model grounded in the finite-element method and equipped with an advanced constitutive model. Furthermore, they validated this numerical model through centrifuge model tests. The model effectively captured essential characteristics of shallow tunnels in partially saturated ground, including the influence of suction on tunnel deformation and stability. Failures of tunnels were frequently triggered by inundation resulting from heavy rainfall or pump failures, and the numerical model was capable of reasonably describing these face failures caused by wetting. It's worth noting that certain uncertainties were inherent in simulating the centrifuge results, such as estimating soil properties, calibrating the constitutive model, and accurately assessing the degree of saturation based on laboratory tests. Nevertheless, the numerical models managed to replicate the responses observed in the model tests quite satisfactorily. As a result, the numerical model presented a valuable tool for tunnel engineers to conduct rational designs for shallow tunnels situated in partially saturated soil.

11. Several tunnels have been constructed around the world and in Egypt to solve the transportation problems such as the Greater Cairo metro and the El-Azhar Road tunnels. These tunnels are considered as major projects in Cairo city. **Sabna and Sankar (2016)** analysed the shallow tunnels in soft ground in Plaxis 2D and compared with these tunnel data. There are technologies to assist in excavation such as tunneling boring machine (TBM), new Austrian tunneling method (NATM), immersed-tube tunneling system, and cut and cover method. Many geotechnical problems were encountered during the construction of the Greater Cairo metro, El-Azhar Road tunnels, and the Greater Cairo sewage tunnel. Most problems are related to the damage of surrounding

buildings due to surface and subsurface ground subsidence. Finite element method is considered as the most appropriate analytical technique to solve geotechnical problems. This thesis presents numerical modeling of a shallow tunnel in soft ground using PLAXIS2D, thus making it possible to evaluate the displacements due to tunneling.

The prediction and mitigation of damage caused by construction-induced ground movements represents a major factor in the design of tunnels. This is an especially important problem for shallow tunnels excavated in soft soils, where expensive remedial measures such as compensation grouting or structural underpinning must be considered prior to construction. Ground movements arise from changes in soil stresses around the tunnel face and the over-excavation of the final tunnel cavity, often referred to as 'ground loss'. Sources of movements are closely related to the method of tunnel construction ranging from a) closed face systems such as tunnel boring machines (with earth pressure or slurry shields), where overcutting occurs around the face and shield ('tail void') while local ground loss is constrained by grout injected between the soil and precast lining system; to b) open-face systems (such as the New Austrian. Tunnelling Method, NATM) where ground loss around the heading is controlled by expeditious installation of lining systems in contact with the soil (typically steel rib or lattice girder and shotcrete) with additional face support provided by a shield or other mechanical reinforcement (soil nails, sub-horizontal jet grouting etc.). In all cases, it is easy to appreciate the complexity of the mechanisms causing ground movement and their close relationship with construction details, especially given the non-linear, time dependent mechanical properties of soils, and their linkage to groundwater flows. This complexity has encouraged the widespread use of numerical analyses, particularly nonlinear finite element methods, over a period of more than 30 years (e.g., review by Gioda & Swoboda, 1999). Although these powerful numerical analyses undoubtedly provide the most comprehensive framework for modeling tunneling processes and interactions with other existing structures (e.g., Potts & Addenbrooke, 1997), their predictive accuracy is also closely tied to the knowledge of in situ conditions and the modeling of soil behavior.

A comparative study of analytical and numerical methods was carried out. Then, model validation was done by comparing with the values drawn from the literature. Construction of shallow tunnels in soft clay can result in significant surface settlements. since tunnel construction often takes place beneath urban areas, engineers are faced

with the problem of predicting these settlements. In most analysis of geotechnical problems, simple elastic or elastic-plastic models are used to represent the behavior of soils. However, in the analysis of shallow tunneling, this implication can result in inaccurate predicted settlement profiles. A more practical model which can account for the realistic behavior of soils is required.

The authors collected data from several case studies, validated the numerical analysis data with the analytical results after constructing the model from field and laboratory tests. The authors studied the settlement behavior of the soil above the tunnel. After that a parametric study has been carried out by the auditors to understand the behavior of the tunnel with the diameter, coefficient of the ground pressure at rest, angle of friction of the ground, effects of Poisson's ratio and angle of dilatancy.

12. In a **2017** study conducted by **Kenichi Soga et al.**, they examined the long-term behavior of tunnels and the associated ground movements in clayey soils following tunnel construction. Over time, ground movements above a tunnel in clayey soils can continue to evolve due to several factors. Initially, the excess pore water pressures generated by tunnel excavation gradually dissipate, contributing to ongoing ground movement. Additionally, the changing earth pressure acting on the tunnel can lead to further tunnel deformation during the consolidation process. The presence of the tunnel itself introduces new drainage conditions, which can vary depending on the drainage characteristics of the tunnel lining. This variation can influence the effective stresses around the tunnel, leading to continued soil consolidation. In many cases, low-permeability clayey soil has a very slow seepage rate, and any groundwater seeping into the tunnel can evaporate quickly. Consequently, even if the tunnel's surface appears dry, the tunnel's drainage conditions may actually be permeable.

The study summarized the investigation of the interaction between soil and tunnel consolidation, with a specific focus on ground surface movements and tunnel lining deformation from an engineering perspective. The analysis results highlighted the significant role played by the tunnel lining's permeability relative to the permeability of the surrounding ground in both long-term ground movements and tunnel lining behavior. The study reviewed findings in the literature, starting from single tunnels and progressing to twin tunnels and complex cross-passage structures. It identified the

mechanisms of tunneling-induced soil consolidation for these structures and proposed potential engineering methodologies for assessing long-term ground surface settlements and tunnel lining loads.

Key findings of engineering importance included:

a) Ground movements could continue to increase after tunnel construction in clayey soil due to the gradual dissipation of excess pore pressure generated during excavation and ongoing soil consolidation influenced by the tunnel's drainage conditions.

b) A method for evaluating long-term surface movements above a single tunnel in clayey soil was proposed, taking into account tunnel drainage conditions, clayey soil compressibility, and excess pore pressures generated during excavation.

c) Horizontal ground strains, crucial for assessing building damage above tunnels, could continue to grow during soil consolidation, reaching magnitudes similar to those induced by tunnel excavation. A method for predicting consolidation-induced horizontal strains was introduced.

d) In both London stiff clay and Shanghai soft soil, metro tunnels typically experience additional settling after construction as the surrounding ground consolidates. The consolidation time for long-term tunnel deformation was significantly shorter than that for ground settlement due to differences in the time it takes to reach quasi-steady state water pressure conditions around and away from the tunnel.

e) Twin-tunnel interaction could increase long-term ground movements, depending on factors such as tunnel excavation-induced shearing, configuration (spacing-diameter ratio), and relative soil-lining permeability. For closely spaced twin tunnels, the soil between them consolidated more rapidly than at the sides, leading to asymmetric long-term tunnel thrust modes. This asymmetry could result in uneven movement of railway tracks due to tunnel lining distortion and rotation.

f) In closely spaced twin tunnels, the presence of cross passages did not appear to increase the magnitude of consolidation-induced surface settlement. However, tunnel stress and deformation accumulated at the cross-passage tunnel opening over the long term as earth pressure redistributed around the structures.

13. An analytical model was proposed by **Liu, Keqi et. al. (2018)**, to predict the horizontal earth pressure at the tunnel face using a silo-ring model. Three-dimensional arching effects and friction between the cutter plates have been considered in this model. The method can be used to evaluate the horizontal soil pressure at the tunnel face and predict the most vulnerable area during excavation. A parametric study was also conducted to assess the influence of cohesion and shearing angle on the horizontal earth pressure, and it was found that, friction angle has more apparent influence than cohesion.

Hence, this model had considered 3D arching effect (making the earth pressure distribution parabolic) and the friction between the cutter and the soil in front of the tunnel face. Then a silo-ring model was proposed to accurately obtain the size and distribution of the earth pressure as well as the maximum value and its position. Cohesion was also seen to have lesser effect on the distribution and size than the friction angle. The results were seen to be in close proximity with the failure mechanism of an actual project.

14. **N. T. Shinde et. al. (2019)** in their paper analysed the tunnel numerically using Plaxis 2D. Their work was aimed to evaluate the location of tunnel depth and effect of existing structure on tunnel by observing the deformation of soil mass while tunnelling. Hence to avoid such ground subsidence and effect of this on surrounding areas many methods are used to determine stresses induced due to such subsidence/settlement. In their study we choose the software Plaxis 2d to analyse the stresses due to subsidence on tunnel. Shown in Fig. 2.1 below are the various parameters they had considered.

Identification	Unit	Lining
Material type		Elastic
EA1	KN/m	1.4E7
EA2	KN/m	1.4E7
EI		1.43E5
W	KN m^2/m	8.40
v (nu)		0.1500

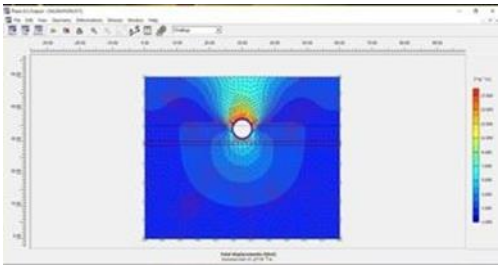

Fig. 2.1 (a) Properties used **(b)** Output window in Plaxis 2D

Using the above input parameter, the initial phase (without clay bed) was modeled and analyzed using PLAXIS and corresponding total displacement was found to be 0.02903m (from the second figure).

The surface settlement during the tunneling and optimum tunnel depth could be based on the analytical, empirical or numerical methods. Present work was aimed to evaluate effect of surrounding soil on tunnel by observing the deformation of soil mass while tunneling. From the above study in the process of completion of this work the conclusion obtain are as follows, for analyze the effects on tunnel, the software plaxis 2d is used. For validation they took previous research paper and compared its values with their validation. The values of their validation are varied within 10-15% of the previous research papers. Hence the software is valid for the analysis of the tunnel. Hence the software can used for further analysis of the effects of surrounding soil and structures on the tunnel.

15. In **2019**, **KunYong Zhang et al.** conducted a three-dimensional finite element analysis using the ABAQUS program to study the interaction between underground pipelines and soil in tunnel construction. They employed PSI elements to simulate the relationship between pipelines and soil. The study involved the analysis of various parameters, including the elastic modulus of the soil, stress release rate, at-rest lateral pressure coefficients, elastic modulus of the pipelines, and the depth at which tunnels were buried. The research aimed to explore the impact of tunnel excavation on the displacement of existing pipelines, establish settlement relationships, and determine the sensitivity of each parameter to surface settlement through grey relational analysis. This analysis provided valuable insights for prioritizing and implementing shield tunneling support methods.

Additionally, the study proposed a formula describing the settlement relationship between the maximum surface settlement and pipeline deformation for different pipe-soil relative stiffness values. This formula was applied in practical cases and compared with field monitoring results and finite element method (FEM) computer simulations. The results showed that the proposed normalized formula closely matched both the measured results and numerical simulations of pipeline settlement.

Key conclusions drawn from the research included:

a) The most influential factor affecting pipeline settlement was the elastic modulus of the soil, followed by the stress release rate, while Young's modulus had the least impact.

b) The formula for pipe-soil relative stiffness, in conjunction with finite element analysis, produced a settlement relationship chart between maximum surface settlement and pipeline deformation. The calculated maximum settlement values from this chart aligned well with the measured results.

c) The study employed a simplified Mohr-Coulomb model for analysis due to its convenience. However, for more sophisticated investigations, advanced models like the cap model should be considered once the required parameters are available.

The application of the grey correlation method in this study revealed significant coefficients related to the constitutive model used. These coefficients could be adjusted for future research employing different advanced constitutive models. Nonetheless, for practical engineering purposes, simpler models with fewer coefficients may be more suitable.

16. Tunnelling in soft ground within urban areas is increasingly employing the shield method, and face stability is a paramount concern due to its profound implications for ground settlement and construction safety. In their **2019** research, **Ahmed S.N. Alagha and David N. Chapman** conducted an extensive series of three-dimensional finite element simulations using the Midas GTS NX software. Their aim was to determine the necessary collapse pressure at the tunnel face during tunnelling, both in homogeneous and layered soil conditions.

In homogeneous ground, they explored the effects of various factors, including different soil strength parameters, cover-to-diameter ratios, and tunnel diameters. From the results of 140 analyses, they derived a novel design equation to calculate the required face collapse pressure for tunnelling in purely frictional soil or a 'c' soil above the groundwater table. This equation closely aligned with experimental and theoretical findings, providing a valuable tool for estimating face collapse pressure. Additionally, they explicitly examined the arching effect and presented failure mechanisms ahead of the tunnel face for various scenarios.

For layered ground, they considered two stratification scenarios, each comprising upper and lower strata. They studied the influence of variations in shear strength parameters of both upper and lower strata on face collapse pressure. Notably, they found that

parameter variations in the lower stratum had a more significant impact on face collapse pressure in Case 1, where the upper stratum intersected with the lower stratum at the tunnel crown. In Case 2, where both strata intersected at the tunnel axis, similar face collapse pressures were obtained for different parameter variations. Furthermore, if the lower stratum was stronger than the upper stratum, Case 2 required a greater face collapse pressure than Case 1.

Key conclusions from their research included:

For Homogeneous Ground:

a) In frictional soils, the relationship between tunnel diameter and face collapse pressure exhibited linearity, with doubling the diameter resulting in a doubling of the collapse pressure.

b) The maximum effect of diameter corresponded with the minimum friction angle, while the minimum diameter effect corresponded with the maximum friction angle.

c) For specific conditions, such as $\varphi' = 20°$ and $C/D = 0.5$, overburden stress did not influence face collapse pressure due to arching.

d) The importance of the arching effect in frictional soil was highlighted for face stability.

e) Under certain tunnel geometries, an increase in friction angle nonlinearly reduced the required face collapse pressure.

f) Cohesion significantly reduced the face collapse pressure, independently of tunnel geometry, but this effect decreased with higher friction angles.

g) The derived equation provided accurate results and can be confidently applied in practice for calculating tunnel face support pressure during shield tunnelling.

h) In frictional soils, the size of the failure mechanism in front of the tunnel face decreased with increasing friction angle.

For Layered Ground:

a) In Case 1, the face collapse pressure was more sensitive to changes in the lower stratum's strength parameters than the upper stratum, while Case 2 showed almost equal sensitivity to variations in both strata.

b) Changes in strength parameters in the lower stratum affected face collapse pressure more in Case 1 than in Case 2.

c) When the lower stratum was stronger than the upper stratum, Case 2 required more support pressure than Case 1.

d) Face support pressure was influenced more by changes in friction angle than cohesion, regardless of variations in upper or lower strata.

e) The soil layer beneath the tunnel invert had no impact on face collapse pressure in the studied cases.

17. In their **2020** paper titled 'Influence of Tunneling in Cohesionless Soil for Different Tunnel Geometry and Volume Loss under Greenfield Condition,' **Raja Kanagaraju and Premalatha Krishnamurthy** presented a numerical analysis of settlement to delineate the vulnerable or influence zone resulting from tunneling activities in cohesionless soil deposits under free field or Greenfield conditions. The analysis took into account several factors, including saturated density (γ_{sat}), unsaturated density (γ_{unsat}), angle of shearing resistance (φ), deformation modulus (E_S), volume loss (V_L), and the support pressure applied at the tunnel face by the shield head. The obtained results from a finite element program (FEM) called PLAXIS 3D were compared with surface settlement measurements and predictions using field instruments, as well as analytical and empirical solutions. The comparisons showed a reasonable agreement, and the predictions were found to be conservative. A minimum ground settlement of 10mm was taken from the literature as the threshold for mapping the influence zone under Greenfield conditions. Structures located beyond this zone were expected to experience negligible settlement.

The paper presented settlement trough characteristics and 10mm settlement contour characteristics for different tunnel sizes at the same depth and the same tunnel size at different depths, respectively. Various influence zones were determined for sandy grounds of varying density based on parametric studies involving tunnel size "D", tunnel axis depth "z," and volume loss "V_L".

The researchers adopted FEM with appropriate soil models and assumptions to address challenges encountered in the instrumentation program. FEM is commonly used to

simulate complex soil-structure interactions and was employed here for three-dimensional finite element analyses to investigate settlement responses resulting from tunneling with different tunnel sizes in various soil conditions and the influence of different parameters on these responses.

The numerical analysis results revealed that different soil and tunnel parameters could be considered for shallow, intermediate, and deep tunneling conditions. Parametric studies were conducted to generate artificial data for plotting influence zones, varying parameters such as tunnel diameter (D), volume loss (V_L), tunnel placement depth (z), and sand density. These numerically derived data, in conjunction with the criteria mentioned earlier, helped determine the influence zones. Engineers can utilize these influence zones to predict vulnerable zones in the field before tunnel construction begins, enabling them to take precautionary measures both before and during tunneling activities to prevent accidents. Future research will focus on the responses of building foundations within these influence zones.

18. In **2020**, **Fan-yan Meng** and colleagues conducted a centrifuge modeling study to investigate the response of the ground and an existing tunnel to a nearby excavation in soft clay. This scenario is commonly encountered in underground construction, but the interaction mechanism, especially in the long term, was not fully understood. Their research involved a three-dimensional centrifuge test using saturated kaolin clay, with a focus on the long-term behaviors of both the ground and the tunnel. They examined parameters such as undrained shear strength, excess pore-water pressure, horizontal earth pressure, compression behavior, settlement, and bending moment.

The study found that the installation of a retaining wall, achieved by statically pressing it into the ground, increased the undrained shear strength of the soil. However, excavation caused a reduction in shear strength, with the final strength depending on their relative magnitudes. Pore pressures below the excavation base initially decreased significantly and then gradually increased over the long term. In contrast, pore pressures above the tunnel crown and near the right springline (close to the excavation) continued to increase, while those near the left springline (away from the excavation) showed a different pattern of increasing, decreasing, and then increasing.

During the excavation stage, horizontal earth pressures on the right side of the tunnel increased with greater burial depth, while pressures on the left side of the tunnel crown were similar to those on the right. After excavation, pressures on the right side of the tunnel experienced a slight initial increase followed by gradual decrease, while pressures on the left side of the tunnel crown showed a continuous and pronounced reduction. These differences in horizontal earth pressure performance were attributed to the presence of the existing tunnel, which altered long-term stress transfer due to the excavation base exposure.

The compressibility of soils on the tunnel side (T_R) was lower than on the other side (E_C), indicating that the existing tunnel influenced the transfer of excavation-induced disturbance. The disturbance degree in terms of compressibility at T_L was mitigated to a greater extent due to the existing tunnel. Similarly, for elevations at the tunnel crown and invert, the variations in compressibility with position implied that the existing tunnel mitigated nearby soil disturbance. However, for soils at the elevation of the tunnel springline, this tendency was reversed.

The ground surface settlement exhibited a concave shape, influenced by factors such as the excavation's length-to-width ratio, the existing tunnel, the stress imbalance between the heavy fluid and horizontal soil stress during the spin-up phase, and the installation of the retaining wall. After excavation, ground surface settlement increased more slowly near the retaining wall compared to areas further from the wall. The increase rate of post-excavation tunnel settlements decreased over time, and tunnel bending moments in both vertical and horizontal directions increased significantly.

Despite these findings, the study had limitations, including the conduct of a single test and the execution of the excavation at 1g. To enhance understanding of this problem, future research should include more extensive parametric studies and realistic excavation modeling. Caution should also be exercised when interpreting the presented data.

19. **Qi et al. (2021)** in this paper presented theoretical methods for the undrained stability analysis of shallow tunnels/sinkholes in clay based on the cavity contraction theory, with some assumptions and simplifications. To examine the accuracy and reliability of the new method, a database was assembled, which consisted of stability numbers of

tunnel/sinkholes in clays from 22 centrifuge model tests, 10 field tests, and 62 FELA results. In order to maintain the stability during shield tunnelling in clays, temporary supports provided by compressed air or slurry were usually necessary. For shield tunnelling in clay, the construction process was usually sufficiently rapid that the clay behaviour around the heading was often regarded as undrained. Since the failure mechanism of a tunnel may be similar to that of a sinkhole, sinkhole stability was also considered in this paper.

To investigate the influence of embedment ratio and tunnel heading geometry on tunnel stability, Mair conducted two series of 2D/3D centrifuge model tests in clays, and found that the tunnel heading stability was strongly affected by the tunnel heading geometry. Following Mair, Wu and Lee studied the tunneling-induced ground movement and collapse mechanisms of single and parallel tunnels, and obtained a series of stability results. Davis, et al. assessed the stability of shallow tunnels using the lower and upper bound theory under plane strain conditions. Using the FELA method, the undrained stability of tunnels under plane strain conditions could be easily determined, even taking the variation of the undrained shear strength into consideration. Later, Augarde et al., Wilson, et al. and Wilson revisited these problems using more advanced FELA techniques and smaller gaps between results obtained, and the lower bound and the upper bound methods were derived. Furthermore, the undrained face stability in clay was also analyzed by the finite element method (e.g., Ukritchon, et al., Huang, et al.), which provided a valuable benchmark for tunnel stability analysis.

This paper mainly took the tunnel collapse as an example in the theoretical analysis and then extended this similar method to the sinkhole stability analysis. The authors first derived the relationship between the internal supporting pressure and the radius of the elastic-plastic boundary. It was shown that the theoretical results derived agree well with numerical results when $H/D \leq 3$ but underestimate the tunnel stability when $H/D = 5$. It meant the tunnel may not collapse when the plastic zone expanded to the ground surface because of the arching effect, and some errors may also be induced from the simplified definition of k parameter.

Fig. 2.2 showed that the experimental results were well contained within the predictions of finite solution and infinite solution. These two analytical solutions were also compared with typical stability numbers computed from lower and upper bound limit analyses.

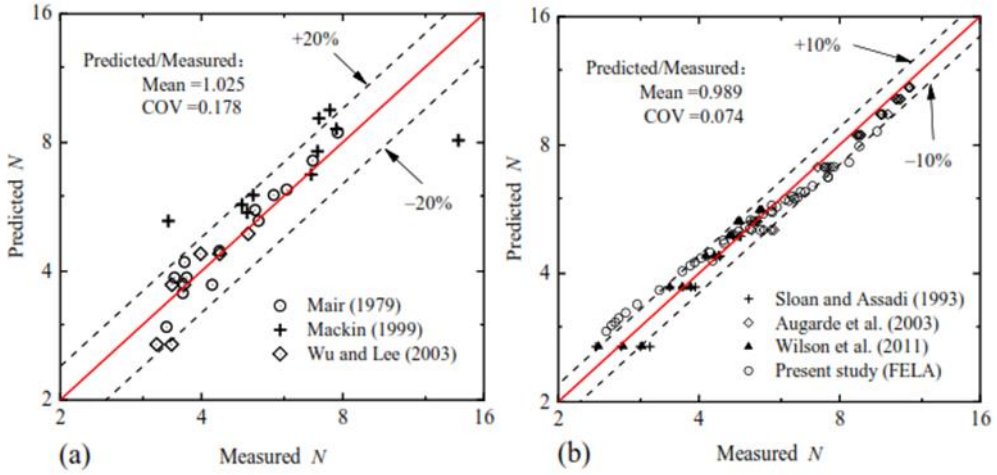

Fig. 2.2 Measured v/s predicted stability numbers: a) model tests and b) FELA results

It was found that the new methods gave a 2.5% overestimation of the stability number when compared with model test results and was in a very good agreement with the FELA results, which suggested that they can be used for the preliminary stability analysis.

2.3 CRITICAL APPRAISAL

After a thorough analysis of the work thus concluded in this field, it can be ascertained that tunneling, as imperative as it is in the transportation industry nowadays, poses many threats. During the review, it was found out that through numerical analysis and laboratory tests, field conditions can be simulated. This in turn would help the engineers to get a vivid image of things. However, not much study has been done on topics covered in this course.

2.4 SUMMARY

A comprehensive range of research papers and journals were examined and are featured in the literature review section. This review encompasses papers related to both numerical analysis and physical testing. From these studies, a thorough evaluation was conducted and summarized. Furthermore, the scope of the research was delineated, taking into consideration

various constraints and limitations. This section serves as a valuable resource for tackling the anticipated challenges in this study.

Chapter 3 : **NUMERICAL MODELING AND METHODOLOGY**

3.1 FINITE ELEMENT ANALYSIS

Finite Element Analysis (FEA) is a computational method employed to approximate and scrutinize complex engineering challenges. It entails breaking down a structure or system into interconnected elements, which serve as representations of the real object's behavior. By employing mathematical models, like governing physical principles or material characteristics, FEA solves a set of equations to replicate and anticipate the system's response under varying circumstances. Through discretizing the issue's domain, FEA can determine stresses, strains, displacements, and other pertinent parameters. This approach empowers engineers and scientists to evaluate the performance, robustness, and longevity of structures, components, and materials. FEA enjoys wide-ranging use in mechanical, civil, aerospace, and automotive engineering, aiding in design enhancement, virtual prototyping, and gaining insights into intricate phenomena.

3.2 PLAXIS; INTRODUCTION

PLAXIS, derived from "**Pl**ane strain and **axis**ymmetric," signifies the specific geometric conditions addressed within its original code. It functions as software in the realm of geotechnical engineering, enabling the execution of finite element analyses (FEA) encompassing deformation, stability, and water flow. Its input procedures simplify the utilization of advanced output features, facilitating a comprehensive presentation of computational results. PLAXIS 3D was developed in 2006 by Brinkgreve and Vermeer, leading to the division of the finite element software into two components: PLAXIS2D and PLAXIS3D. While PLAXIS2D excels in handling plane-strain and axisymmetric issues, PLAXIS3D is more adept at faithfully replicating site conditions in FEA.

PLAXIS primarily serves as a practical analysis tool for geotechnical engineers. Its adaptability is evident in the inclusion of diverse features such as Geogrids, embedded beams, ground anchors, and tunnels, rendering it a highly flexible and comprehensive geotechnical software package. Additionally, it incorporates various soil models, including Mohr-Coulomb and the Hoek-Brown model, as well as advanced soil models like soft soil, hardening soil, and soft soil

creep, among others. This enables the simulation of soil behavior observed in real-world field conditions.

3.3 GENERAL DESCRIPTION OF THE SOIL AND THE TUNNEL

To study the behaviour of tunnel and its ground interactions, it becomes imperative to adopt a soil profile and create a tunnel section with subsequent stages and loading, in order to study the deformation of the ground.

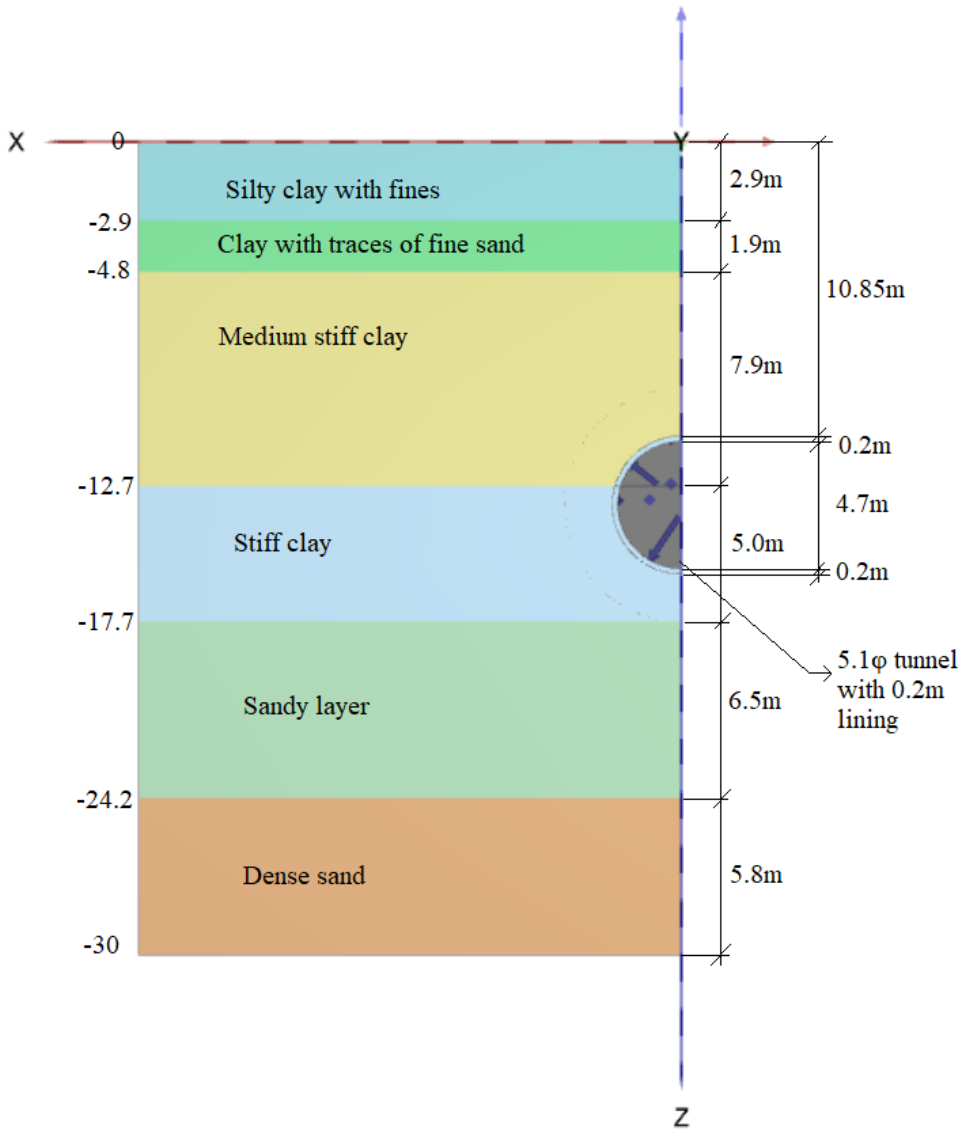

Fig. 3.1 Representative soil profile

Fig. 3.1 illustrates a schematic diagram showcasing the soil profile and the tunnel section. The soil profile considered is a typical Kolkata soil profile. The top 2.9 m consists of silty clay with fine grained soil. The next 1.9 m shows a change in properties with the fines amount decreasing slightly, followed by medium stiff and stiff clay layer spanning for 7.9 m and 5 m respectively.

Then sand layers are encountered for the rest of the strata with denser soils at greater depths. Corresponding properties of each of the soils are going to be mentioned in the subsequent sections. However, those properties have somewhat been changed to get a clarity in the results. The tunnel section considered is of 5.1 m diameter, which includes 0.2 m of lining of concrete. The properties of the lining will also be discussed under the next sub-headings. Detailed discussions are going to be covered in the upcoming parts.

3.4 USE OF PLAXIS 3D FOR THE PRESENT STUDY

The numerical simulation of the tunnel entails several critical input parameters, including soil layer characteristics, liner properties, TBM specifications, necessary pressures for tunnel stability, and the staged construction approach. PLAXIS 3D V20, a finite element analysis software, was utilized for this simulation. The process unfolds in a step-by-step manner, commencing with the selection of soil parameters and the subsequent creation of an appropriate tunnel geometry. Tunnel attributes such as cross-section, trajectory, and construction sequence are then determined. Once these parameters are established, meshing is performed with the desired level of precision. Due to the complexity of the calculations, only half of the tunnel is simulated. Finally, the calculation type is specified, and the analysis is executed to produce the desired results.

3.4.1 *Soil Model and properties*

The material properties of different materials used for the numerical study have been furnished in Tables 3.1 and 3.2.

Table 3.1 Parameters used for the soil and lining material

Materials	**Material Model**	**Saturated Unit Wt. γ_{sat} (kN/m^3)**	**Unsaturated Unit Wt. γ_{unsat} (kN/m^3)**	**Drained angle of friction, ϕ' (°)**	**Drained cohesion, c' (kPa)**	**Drained Elastic Modulus, E' (kPa)**	**Drained Poisson's Ratio, ν'**
Silty clay	Mohr Coulomb	16	15.8	26	0	5000	0.35
Clay with traces fines	Mohr Coulomb	18	17.8	27	0	10000	0.35
Medium stiff clay	Mohr Coulomb	17	16.9	26	0	10000	0.35

Stiff clay	Mohr Coulomb	19	18.8	25	10	20000	0.35
Sandy layer	Mohr Coulomb	20	19.8	32	0	25000	0.30
Dense sand	Mohr Coulomb	20	19.8	36	0	30000	0.30
Concrete	Linear Elastic	-	27	-	-	$3.1E10^7$	0.10

Table 3.2 Material Properties of the plate representing the TBM

Parameter	**Name**	**TBM**	**Unit**
Type of behaviour	-	Elastic; Isotropic	-
Thickness	d	0.17	m
Material weight	γ	247	kN/m^3
Young's modulus	E_1	$200E10^6$	kN/m^2
Poisson's ratio	ν_{12}	0	-
Shear modulus	G_{12}	$100E10^6$	kN/m^2

The values specified in Table 3.1 represent the parameters that have been modified for this study. It's important to note that there are other parameters that have not been discussed, and for all these remaining parameters, the default values provided by Plaxis 3D are utilized. Additionally, it's worth mentioning that this project exclusively focuses on investigating the long-term effects. Consequently, all soil layers are defined as 'Drained' during the soil characterization phases. This choice ensures that no excess pore pressures are generated, making it possible to simulate long-term soil behaviour without the necessity of modelling the precise loading and consolidation history, which is typically undrained.

Moreover, it's essential to highlight that the PLAXIS 3D Tunnel program does not offer the capability to explicitly model primary consolidation. Therefore, the drained case is employed as an approximation to estimate consolidation settlements. The software developers assert that the results obtained from the drained analysis closely align with what a consolidation analysis

would yield. Furthermore, taking undrained behaviour into account significantly complicates the analysis.

Regarding concrete, the drainage parameter is configured as 'Non-porous'. The material used to represent the Tunnel Boring Machine (TBM) is necessarily composed of steel, and its specific values can be found in Table 3.2.

3.4.2 *Model Configuration*

The model consists of a tunnel having its centre at a depth of 13.4 m. as mentioned earlier, for simplicity, only half of the tunnel is taken into consideration with the Z-axis acting as the line of symmetry. This reduces the number of calculations, the number of nodes and elements to half of what should have been for the whole tunnel. The top of the tunnel is at an elevation of -10.85 m (Fig. 3.1). The lining thickness is 0.2 m bearing the characteristics as mentioned in Table 3.1. An isometric view of the whole model is been shown is Fig. 3.2. The soil block spans 80 m in the positive Y-direction, 20 m in the negative X-direction. The vertical extent of the soil block is 30 m in the negative side.

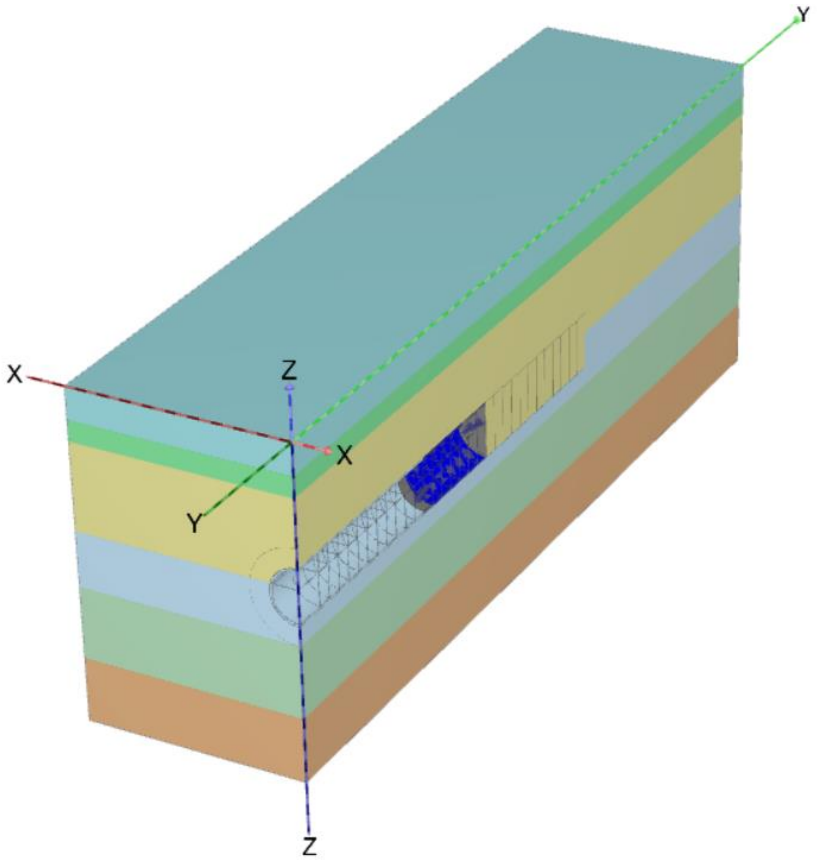

Fig. 3.2 Isometric view of the model

3.5 METHODOLOGY

The research methodology primarily centers around utilizing numerical techniques to examine the tunnel-soil system. Advanced geotechnical software, namely PLAXIS 3D, was employed for conducting numerical simulations to mimic how the soil layers respond to tunneling activities. To capture the intricate interplay between the soil and the structure, the Finite Element Method (FEM) was employed. In a broader context, the process of numerical analysis was subdivided into five distinct categories:

a) Soil
b) Structures
c) Mesh
d) Flow Conditions
e) Staged Construction

A shield tunnel's lining is made of prefabricated concrete segments bolted together within a stationary tunnel boring machine (TBM). The construction process is divided into 1.5 m stages, with each stage involving repetitive steps. To model this, slices of 1.5 m length are used. Each phase represents various aspects of excavation, including support pressure, TBM shield shape, soil excavation, lining installation, and gap grouting. Input remains the same for each phase, except for its shifted location, which moves by 1.5 m each time.

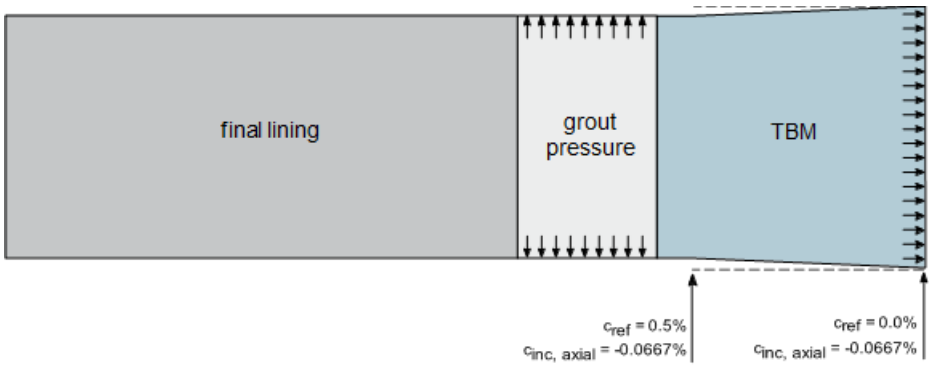

Fig 3.3 Construction stages of a shield tunnel model

As shown from Fig. 3.3, the shape of the TBM is slightly of cone type. Typically, the cross-sectional area at the tail of the TBM is about 0.5% smaller than the front of the TBM. The reduction of the diameter is realized over the first 7.5 m length of the TBM while the last 1.5 m to the tail has a constant diameter. This means that the section tail has a uniform contraction of 0.5% and the remaining 5 sections have a linear contraction with a reference value C_{ref} = 0.5% and an increment $C_{inc,axial}$ = -0.0667%.

3.5.1 *Soil*

The process of numerical modeling commences with the establishment of the soil profile. This involves the incorporation of materials and the assignment of their corresponding characteristics. The characteristics of the soil, concrete, and TBM are detailed in Tables 3.1 and 3.2, respectively. As depicted in Figure 3.1, the properties are allocated to define the soil profiles. Creation of a borehole is then done at the origin point, and the strata are defined as shown in Fig. 3.4.

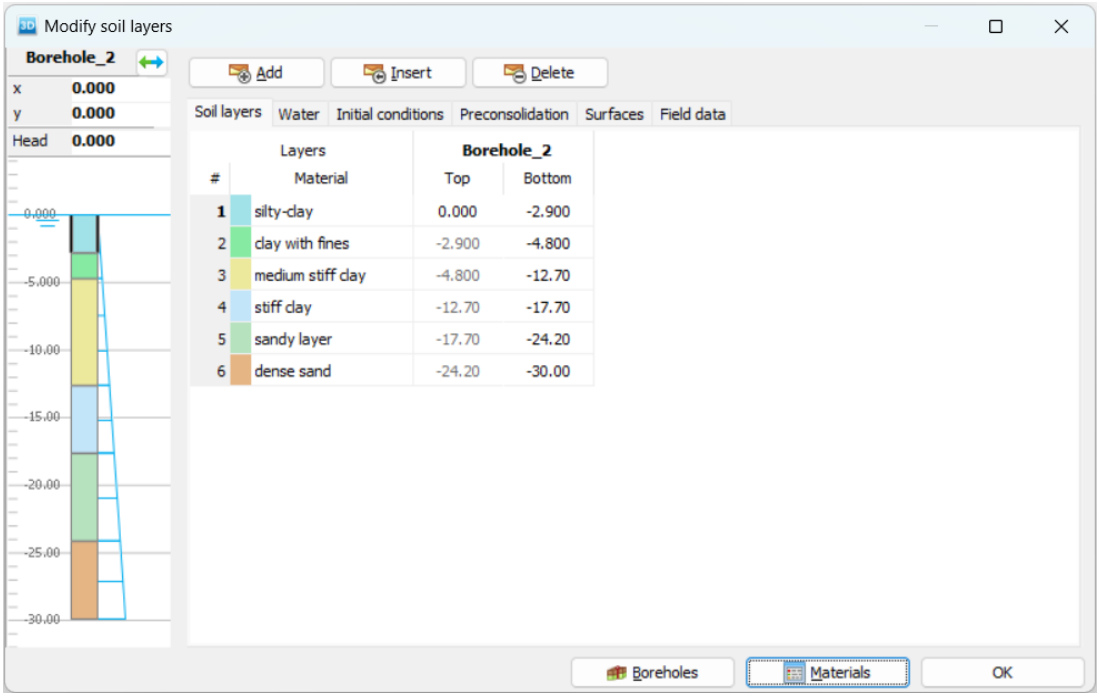

Fig. 3.4 Creation of the bore hole

Nonetheless, a crucial aspect to bear in mind during this procedure is the choice of a suitable soil model. The predominant and widely employed soil model is the Mohr-Coulomb model.

Mohr coulomb: Soils demonstrate non-linear responses when exposed to variations in stress or strain. The stiffness of soil is influenced by several factors, including the level of stress, the path of stress, and the extent of strain. Advanced soil models within PLAXIS incorporate these elements to capture the intricate behaviour of soil. However, for an initial approximation of soil behaviour, the Mohr-Coulomb model is widely employed due to its simplicity and well-established characteristics.

The Mohr-Coulomb model can be described as a linearly elastic perfectly plastic model. The linear elastic portion is based on Hooke's law of isotropic elasticity, which is represented by

Young's Modulus (E) and Poisson's ratio (ν). The perfectly plastic component is derived from the Mohr-Coulomb failure criterion.

In the field of geotechnical engineering, the Mohr-Coulomb soil model is utilized to describe soil behaviour. It employs cohesion (c) and the angle of internal friction (φ) to characterize shear strength. This model establishes a relationship between shear stress (τ) and normal stress (σ_n) through a specific equation.

$$\tau = c + \sigma_n \tan \varphi \tag{3.1}$$

When the applied stresses exceed these values, the soil experiences shear failure. Despite its simplicity, the model is widely applied in various engineering analyses.

3.5.2 *Structures*

The tunnel excavation is carried out by a tunnel boring machine (TBM), which is 9 m long. The TBM has already advanced 3 m into the soil and subsequent phases will model 1.5 m advancement each. The process commences by creating the tunnel section, by clicking the *Start designer* and then the *Create tunnel button*. The lowest point of the tunnel (in our case (0 0 -15.75)) is mentioned, in the *Selection explorer*. In the *General* tabsheet of the *tunnel designer*, *Circular* is selected. As only half of the tunnel is to be designed, *Define left half* is selected. Then in the *Segments* tabsheet, radius is set to 4.7 m and a thick lining of 0.2 m is given

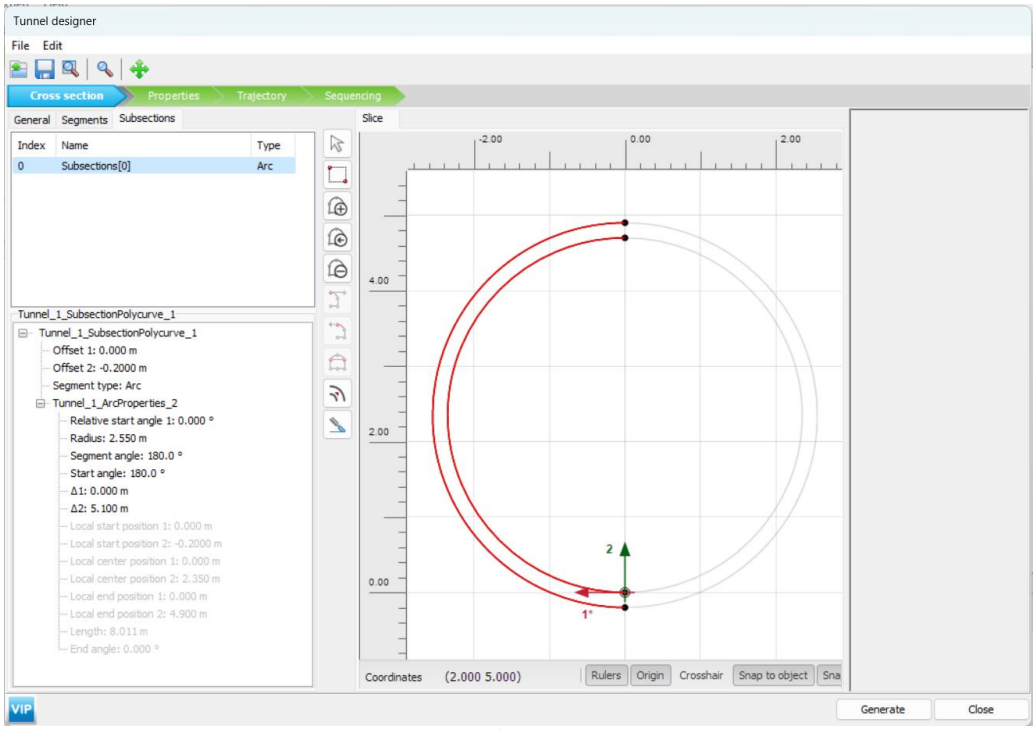

Fig. 3.5 Preview of the tunnel section

throughout in the *Generate thick lining*. A preview of the generated tunnel is as shown in Fig. 3.5.

Now, in the *Properties* tabsheet, properties such as grout pressure, surface contraction, jacking forces and tunnel face pressure are defined. A plate is created by right-clicking the outer surface and material properties given in Table 3.2 are assigned to it. Then *Create negative interface* is selected by right-clicking on the outer surface. To provide surface contraction, *Create surface contraction* is selected. *Axial increment* is opted for and C_{ref} and $C_{inc,axial}$ are defined as 0.5% and -0.0667% respectively. Negative value denotes decrease of contraction in the positive Y-direction.

The next step is to define the grout pressure. It is the surface load which is constant during the building process. A shown in Fig 3.3, it acts at places where soil isn't lined. It provides stability to the upper layers and prevents its failure by acting in the radial direction. *Create surface load* is selected by right-clicking on the outer surface and *Perpendicular, vertical increment* is selected for distribution. $\sigma_{n,ref}$ and $\sigma_{n,inc}$ are set at -110 kN/m^2 and -20 kN/m^2/m respectively. Reference point is set as (0 0 -10.65).

Tunnel face pressure needs to be provided for. The tunnel face pressure is a bentonite pressure (Bentonite Slurry, BS) or an earth pressure (Earth Pressure Balance, EPB) that increases linearly with depth. For the initial position of the TBM and the successive positions when simulating the advancement of the TBM, a tunnel face pressure has to be defined. In the *Plane* tabsheet, *Create surface load* is selected again, by right-clicking on both the selected surfaces. The Distribution is set to Perpendicular, vertical increment and $\sigma_{n,ref}$ and $\sigma_{n,inc}$ are set at -110 kN/m^2 and -16 kN/m^2/m respectively, keeping the reference point same.

In order to move forward during the boring process, the TBM has to push itself against the existing tunnel lining. This is done by hydraulic jacks. The force applied by the jacks on the final tunnel lining has to be taken into account. This will be assigned to the tunnel lining in *Sequencing* tab.

The next step is to create the path of the boring process. The TBM already advanced 3 m into the soil and then proceeds till 48 m excavating slices of 1.5m each. Two segments are created one of 3 m and the other of 48 m. The slices are created by setting the Slicing method as Length, and giving it as 1.5 m. Next comes the *Sequencing* tab.

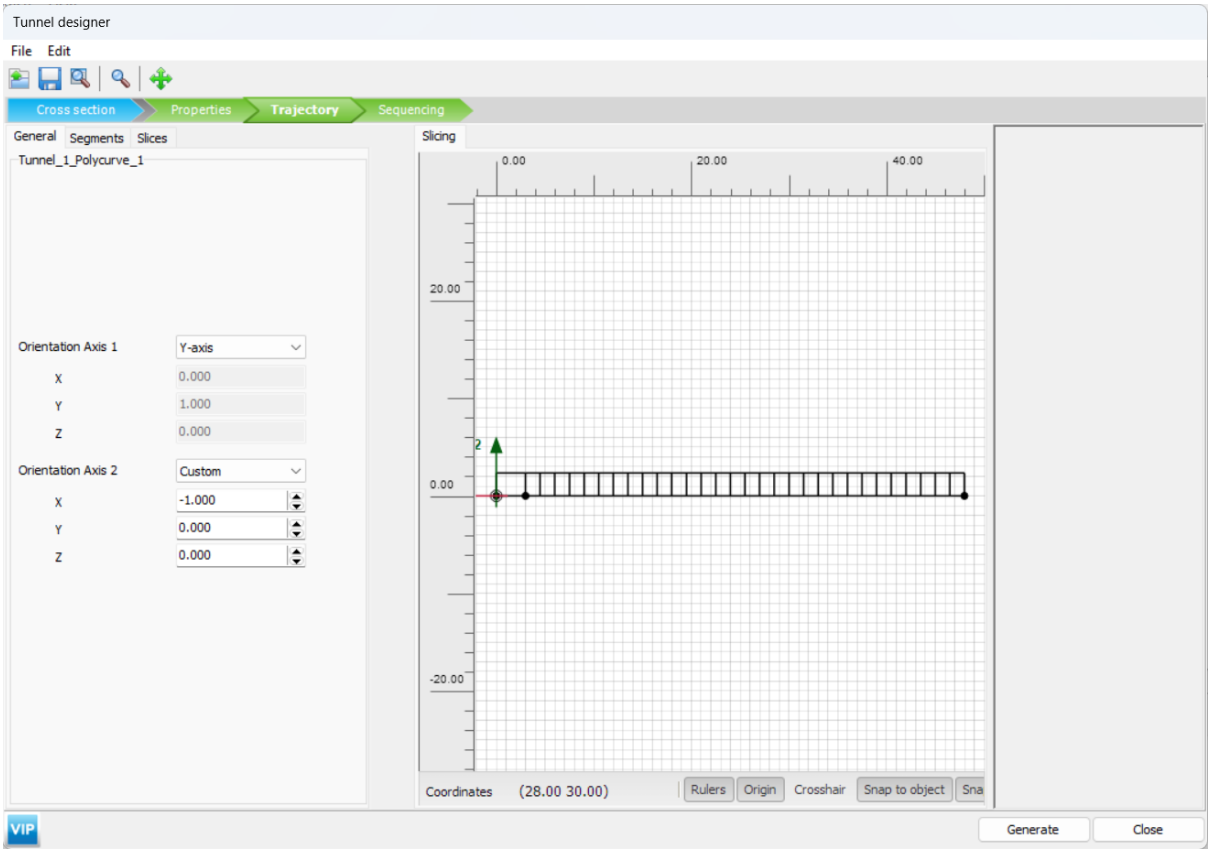

Fig. 3.6 *Trajectory* tabsheet in the *Tunnel designer*

In order to simplify the definition of the phases in *Staged construction* mode, the sequencing of the tunnel is defined. The soil in front of the TBM will be excavated, a support pressure will be applied to the tunnel face, the TBM shield will be activated and the conicity of the shield will be modelled, at the back of the TBM the pressure due to the back fill grouting will be modelled as well as the force the hydraulic jacks driving the TBM exert on the already installed lining, and a new lining ring will be installed. Firstly, the *Excavation method* as *TBM* in the *Sequencing* tab. Total eight steps are required for the whole process. The first 6 steps will have an increasing surface contraction value, starting from 0% to 0.5%. The seventh step will include deactivation of the surface contraction, negative interface and the plate and activating surface load corresponding to the grout pressure. Then, surface load corresponding to jacking thrust is also defined, in the *Plane rear* tabsheet. *Perpendicular* option is selected for the distribution with $\sigma_{n,ref}$ = 635.4 kN/m^2 . Then the final step involves activating the negative interface, but deactivating the grout pressure. The outer volume is also activated, and *Concrete* option is selected. Also, the force of jacking is deactivated. *Generate* option is then pressed to include the defined tunnel in the model. After creation, the *Structures* mode window will look like as shown in Fig. 3.7.

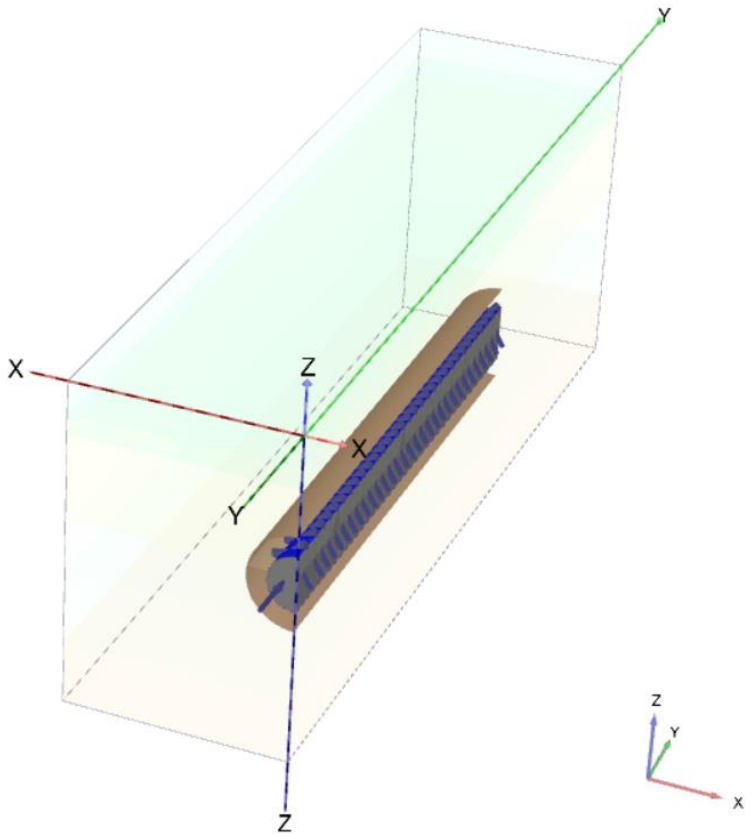

Fig. 3.7 The created tunnel in the *Structures* mode

3.5.3 *Mesh*

As previously mentioned, the numerical model utilized in this study employs 10-noded tetrahedral elements for discretizing the soil volume. In order to achieve a compromise between computational efficiency and precision, a very fine mesh refinement was chosen. This choice was made with the aim of attaining a high level of accuracy in node placement.

By judiciously adjusting the level of mesh refinement, the numerical model effectively balances computation time and accuracy. This approach permits a finer analysis in critical regions of interest, such as the interface between the tunnel and the soil, while still maintaining computational efficiency in other areas. This methodology facilitates the acquisition of dependable and comprehensive results concerning the behaviour of both the soil and structures under various loading and boundary conditions. Consequently, it enhances our comprehension of the overall system response and enables more informed engineering decisions to be made. The mesh generation window and the generated mesh are shown in the Fig. 3.8.

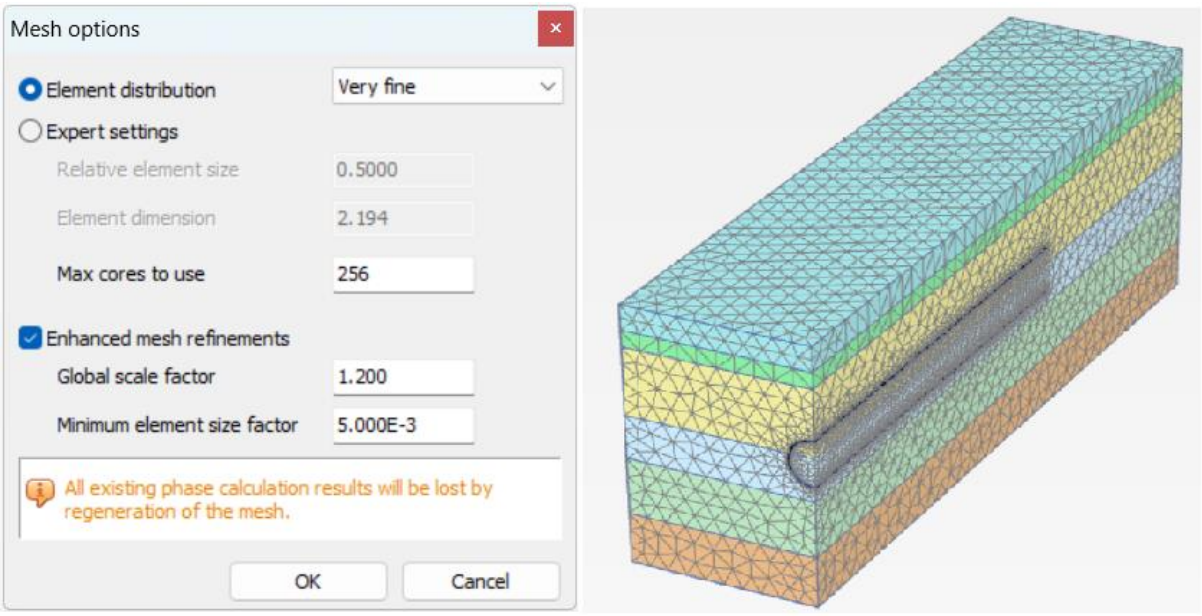

Fig. 3.8 (a) Mesh generation window; **(b)** Generated mesh with required mesh refinement

3.5.4 *Flow Conditions*

Since water levels remain constant the Flow conditions mode can be skipped.

3.5.5 *Staged Construction*

The excavation of the soil and the construction of the tunnel lining will be modelled in the Staged construction mode.

The initial stage distinguishes itself from the subsequent phases in that it marks the activation of the tunnel for the very first time. During this initial phase, the tunnel has progressed 3 meters into the soil. In contrast, the succeeding phases will depict a progression of 1.5 meters each time.

Initial phase: The initial phase consists of the generation of the initial stresses using the K0 procedure. The default settings for the initial phase are valid.

Phase 1: In this phase, the tunnel is considered to have advanced 3 m. For doing this, we add a phase and set the Advancement step to 7, by expanding Tunnels and then Tunnel_1. Also, the plates representing the TBM are activated and 0.5% contraction is applied. Then the soil volume corresponding to the first 3 m is deselected and plates and uniform contraction are active. And the surface load corresponding to the jack thrusting is deactivated, because the TBM is only placed in this phase and it's not moving. Fig. 3.9 shows the preview of the tunnel after the Phase 1.

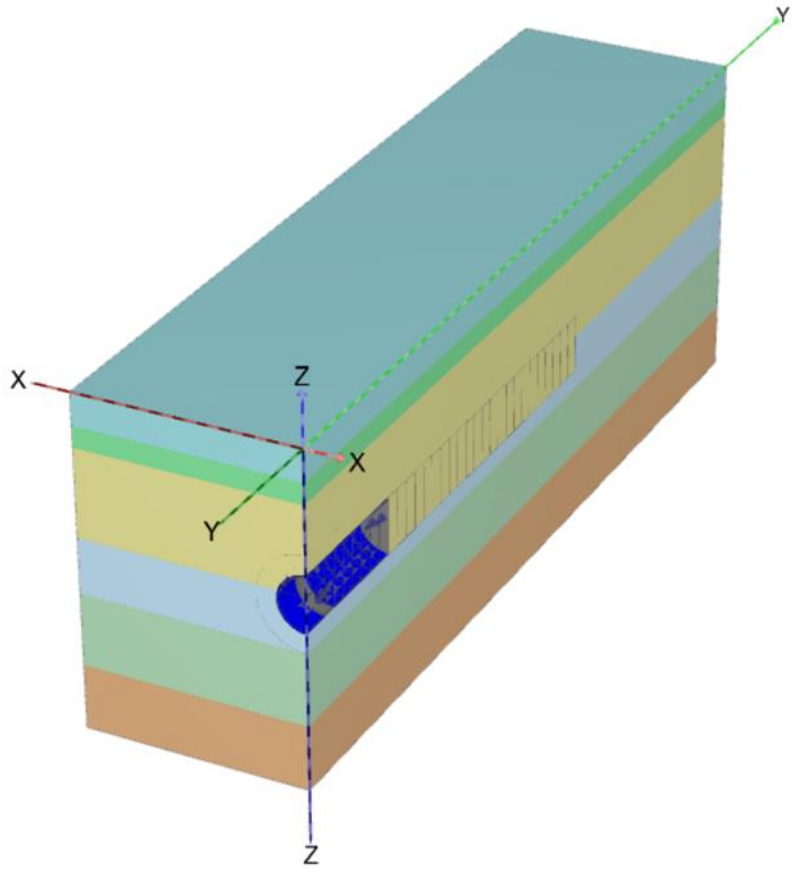

Fig. 3.9 Preview of Phase 1

Phase 2: The next advancement of the tunnel (i.e., y= 13.5 to y=15) is being done. To do this, *Advancement step* is set to 8. Preview of the phase is shown in Fig. 3.10.

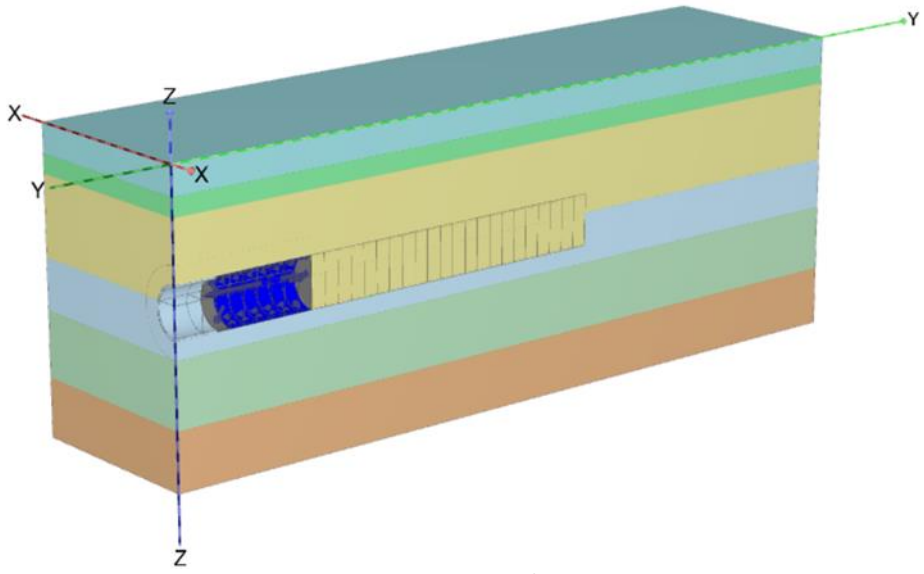

Fig. 3.10 Preview of Phase 2

Phase 3: Here the tunnel advances from y=15 to y=16.5. For this, the *Tunnels* is expanded, and *Advance to next tunnel step* is clicked on, by right-clicking on *Tunnels_1*.

Subsequent steps are done in the similar fashion, until the tunnel has already advanced to y=48 m. To start the calculation, *Calculate* button is pressed by ignoring the "No nodes or stress points selected for curves" message. After calculations are completed, *View calculation results* is pressed to go to the output window. Preview of the final phase viz., phase 24, in the output window, is shown in the Fig. 3.11. Further analysis can be done from there, from the deformations or stress drop-down menus as required for the study. Sections, lines can be cut in the model as deemed fit, for analysis purpose.

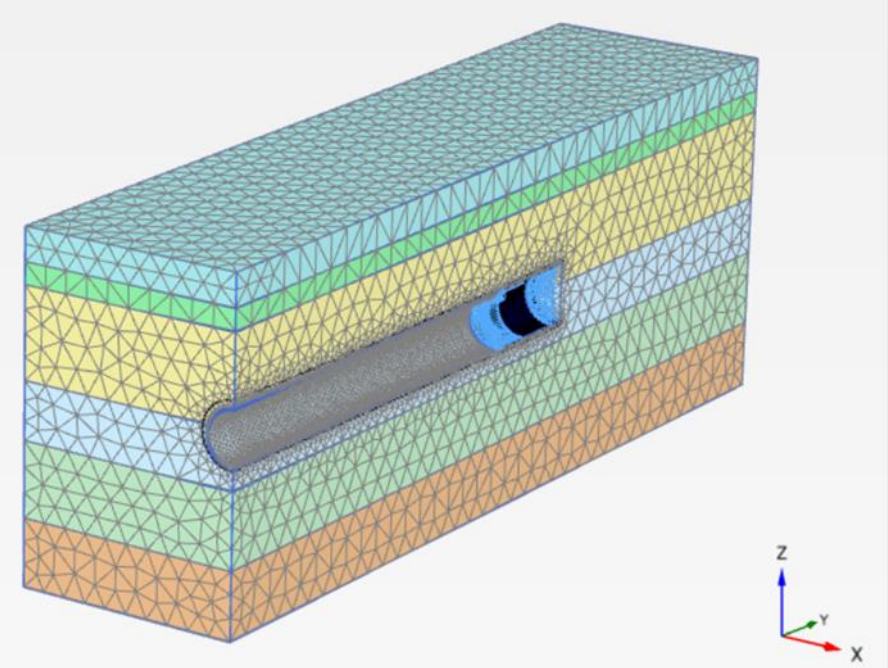

Fig. 3.11 Preview of phase 24 in the output window

3.6 TEST PROGRAM

The principal goal of this research was to pinpoint and examine the primary factors that had the most substantial impact on the interaction between tunnels and the surrounding soil. To fulfill this aim, we conducted a thorough investigation that encompassed the examination of various deformation patterns in the soil profile as the tunnel advanced.

Initially, the deformations of the ground surface are to be studied with tunnel advancement. Deformations on the ground surface include-

1. Cross-sectional profile at a particular value of Y (33.7 m), with the different stages of tunnel advancement.
2. Longitudinal profile at ground level, for different phases of the tunnel advancement.
3. Deformation ILD at three different values of Y (25.3 m, 29.5 m, 33.7 m), for the different phases.

In order to justify the obtained shapes, stresses variations with depths are plotted. Stresses include σ_{xx}, σ_{yy}, σ_{zz} which are plotted against the Z-coordinates for two different values of Y (25.3 m, 33.7 m). Stress paths for those two sections are also plotted in order to understand the ground deformation patterns. Mohr's circle for one such Y (33.7 m) are also drawn for three different depth (10.8 m, 8.86 m, 6.67 m) and changes with phases are noted. All these studies are done at the tunnel centerline i.e., above the tunnel center.

Another separate study involves, analysis of the ground loss. Ground loss becomes a very important part of ground-tunnel stability study. It determines whether or not, the tunneling will provide the requisite safety of the ground and the structures built above. A particular point is to be selected along the Y-direction (33.7 m). Analysis is to be done for a particular stage of tunnel head position (phase19). The difference in volume of the tunnel inside the actual lining, and the final lining (due to the pressure of the soil above) is to be noted. And that difference is expressed as a factor of the volume of ground subsidence. This factor gives an overview of the stability that can be expected from the system. The above-mentioned topics will be addressed in this brief study.

Chapter 4 : **RESULTS AND ANALYSIS**

4.1 INTRODUCTION

Numerical analysis was conducted using Plaxis 3D and the model was created as mentioned in Chapter 3. Investigations were conducted utilizing Mohr-Coulomb's criterion to account for elasto-plastic behaviors of the assembly. The tunnel advancements are shown as different phases. For instance, when the tunnel is in Phase 1 condition, it has already cut through the first 4.5 m of the soil, and it is stayed at the stretch of 4.5 m – 13.5 m. But the lining is done for the first 3 m only, with the next slice (3 m – 4.5 m) being stabilized by grout pressure. The detailed Phase, Tunnel head and the Liner position relations could be understood from Table 4.1, given below.

Table 4.1 Tunnel position details

Phases	Tunnel position (m)	Liner position (m)
1	13.5	3
2	15	4.5
3	16.5	6
4	18	7.5
5	19.5	9
6	21	10.5
7	22.5	12
8	24	13.5
9	25.5	15
10	27	16.5
11	28.5	18
12	30	19.5
13	31.5	21
14	33	22.5
15	34.5	24
16	36	25.5
17	37.5	27

18	39	28.5
19	40.5	30
20	42	31.5
21	43.5	33
22	45	34.5
23	46.5	36
24	48	37.5

Deformations, stresses or any other parameters are going to be calculated and presented for all of these phases. However, sometimes for simplicity and for avoiding over-congestion, alternate or alternate-to-alternate phases might have been graphed to study the variations.

4.2 DEFORMATION PROFILE

Tunneling action in any soil results in deformation of the soil-strata overlying it. This is due to the stresses acting and its re-distribution. However, the deformation isn't of an arbitrary nature but follows some fixed pattern. In this chapter we will discuss some of the deformation profile and try to analyze it further.

4.2.1 *Face deformation*

Here, we fix a particular coordinate along the Y-axis and a cross-section is taken at that point. The coordinate under focus here is 33.7 m in the positive Y-direction. Using the vertical cross-

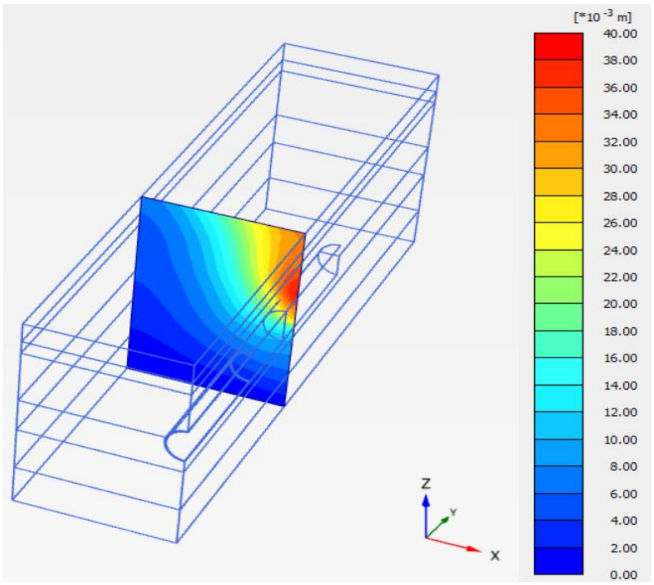

Fig 4.1 Cross-section of the model at 33.7 m

section option in the output window, we create the cross-section with (0, 33.7) and (-20, 33.7) as the first and second point respectively. The section will look as shown in Fig. 4.1. Then the *Table* button is pressed to get a list of deformation values at different nodes in that section.

This is done for all the phases, separately, and the net result is plotted in the form of a graph. The graph will have distances in the X-coordinate and deformation of the ground surface corresponding to that value of X (negative values according to the coordinate system). Fig. 4.2 gives a representation of the same. Last phase has been purposefully left out, as that was superseding the Phase 23 line.

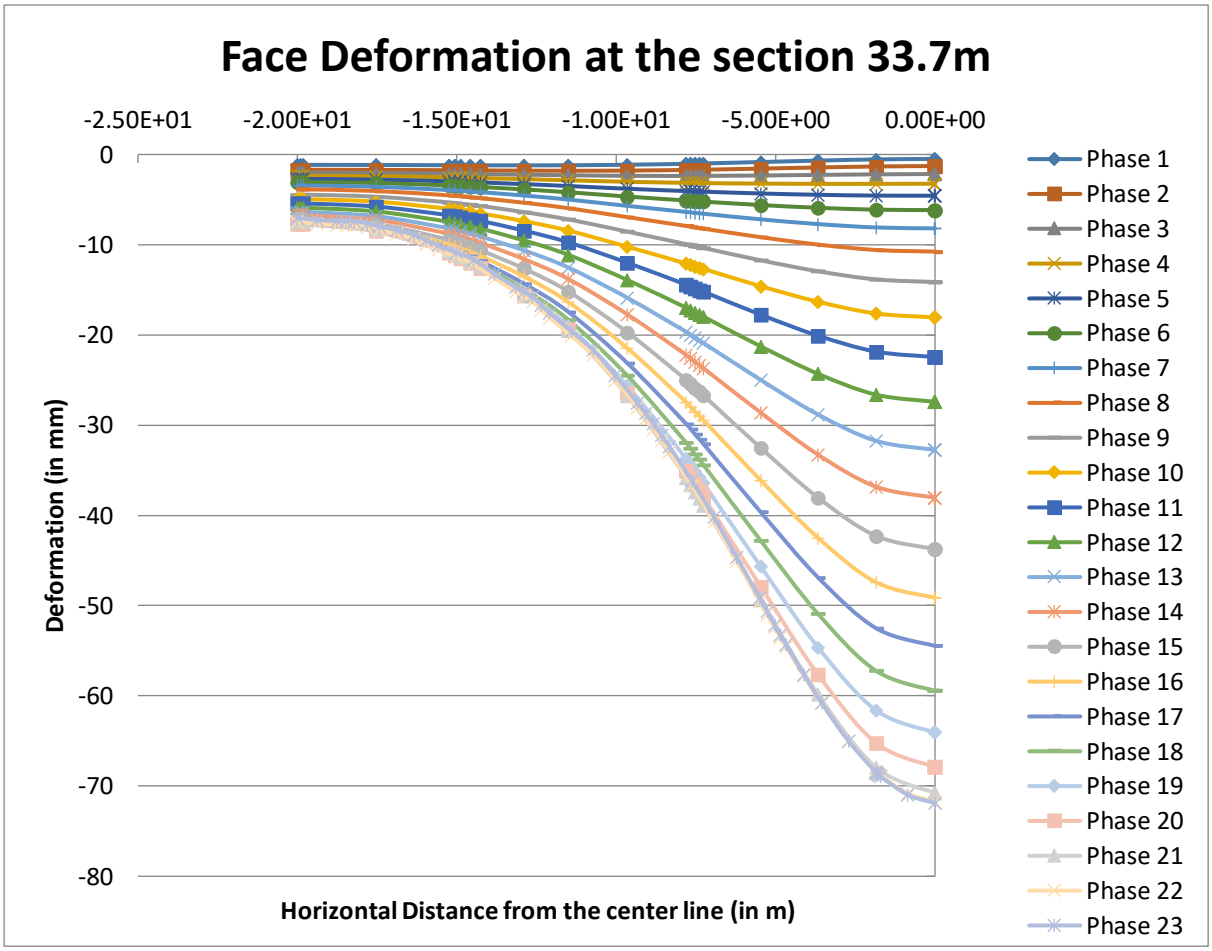

Fig. 4.2 Face deformation at 33.7 m section

The section which is under study, is being crossed by the tunnel in-between phases 14 and 15. Initially, the deformed shapes were seen to be close to one other. The gaps went on increasing as the tunnel advanced further. Then it assumed an approximate maximum in-between phase 14 and 15, or, 15 and 16, where the tunnel crossed the section. But after that it again started decreasing, as the tunnel advanced. More-so-ever it started getting overlapped in the phases 22 and 23. A little rebound was also seen to happen in the last phase. This may be attributed to the soil model that has been chose, which will be discussed in detail in the upcoming sections.

4.2.2 *Longitudinal deformation*

To study the longitudinal deformation, a line is to be selected from the *Line cross section* option appearing in the output window. In the window that has opened, coordinates to be given are (0, 0, 0) and (0, 80, 0). This basically denotes the line on the ground surface along the longitudinal axis of the tunnel. Fig. 4.3 shows the total displacement of the line for a particular phase.

Getting this done for all the phases, we get the values which can be used to draw a pattern of the longitudinal displacements. Fig. 4.4 represents the longitudinal profile of ground level settlement for all the phases. Line for phase 1 has been omitted due to inconsistency in the results. The maximum settlement is approximately seen to lie at points in-between the liner position and where the grout pressure acts. And this is valid for all the phases independently. However, phase 5 onwards, some rebound of the soil or up-heaving of the soil is also seen to take place. This may be attributed to stress re-distribution or factors which will be discussed in the upcoming sections.

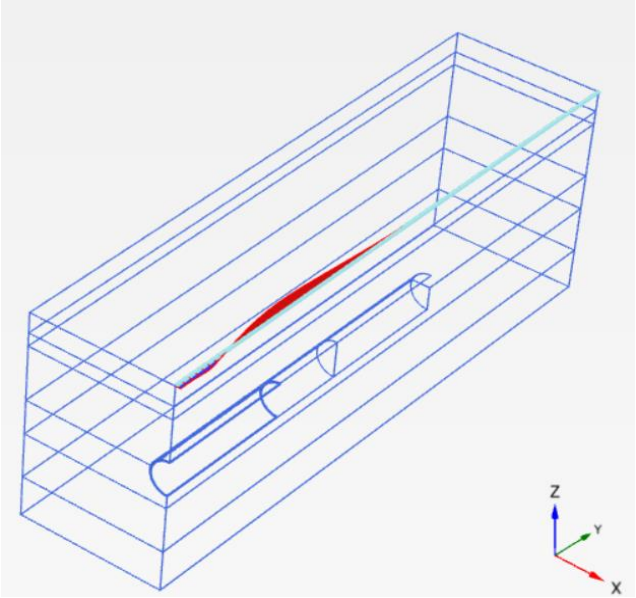

Fig. 4.3 Line under consideration on the ground surface

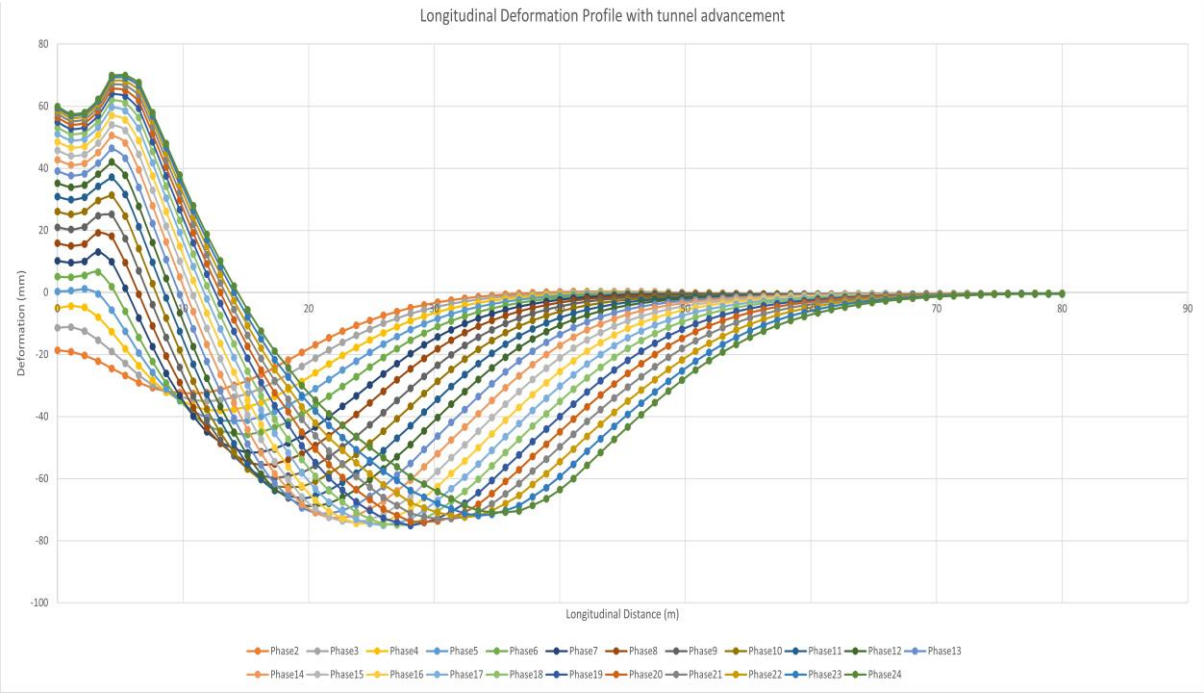

Fig. 4.4 Longitudinal displacement profile of the line for the different phases

4.2.3 *Deformation ILD*

ILD is the abbreviation for Influence line diagram. It is basically study of a function (in our case, deformation) at a particular point with a moving load or a dynamic object. The deformation of a particular point is studied as the tunnel advances. Here the analysis is done at three different points, viz., 25.3 m, 29.5 m, 33.7 m. So, we get three different ILDs and deformation for each of the phases is denoted in them. Fig. 4.5, 4.6, 4.7 denote the ILDs for 25.3 m, 29.5 m, 33.7 m, respectively, on the ground surface.

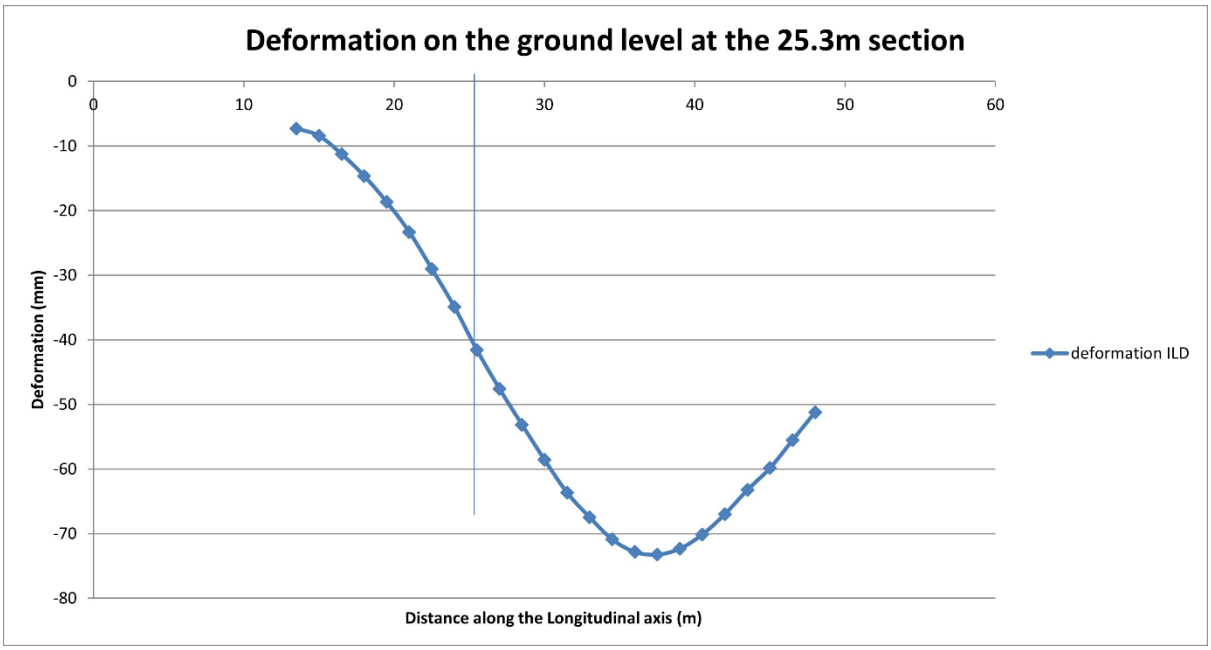

Fig. 4.5 Deformation ILD at 25.3 m section on the ground surface

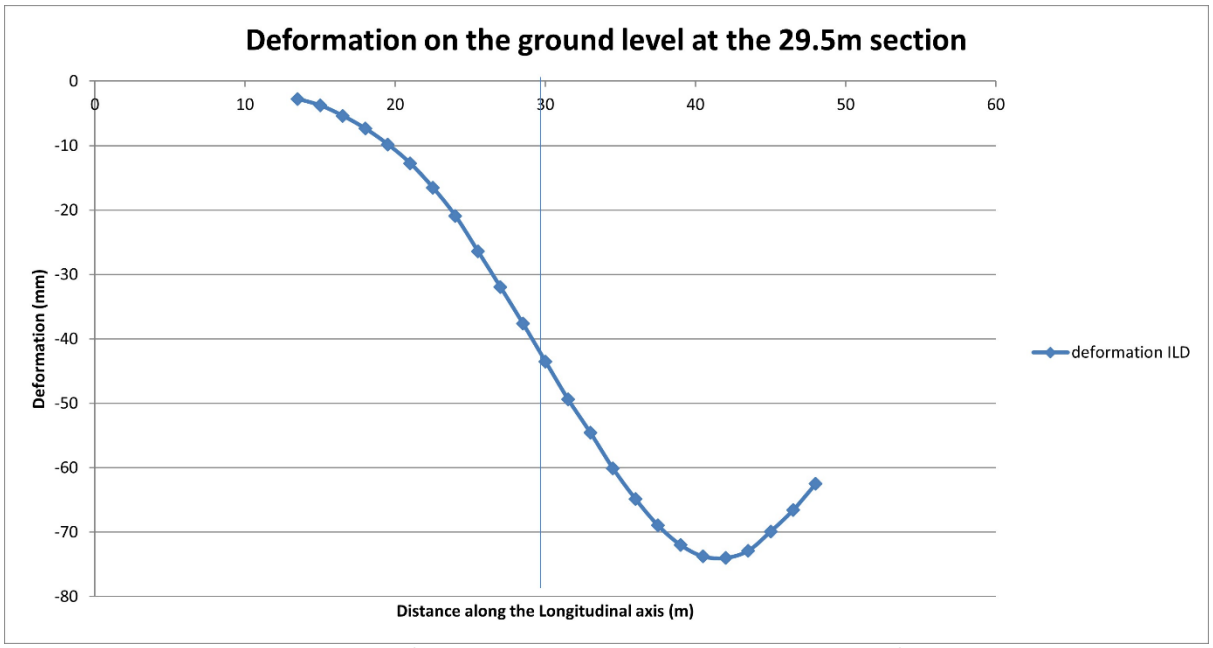

Fig 4.6 Deformation ILD at 29.5 m section on the ground surface

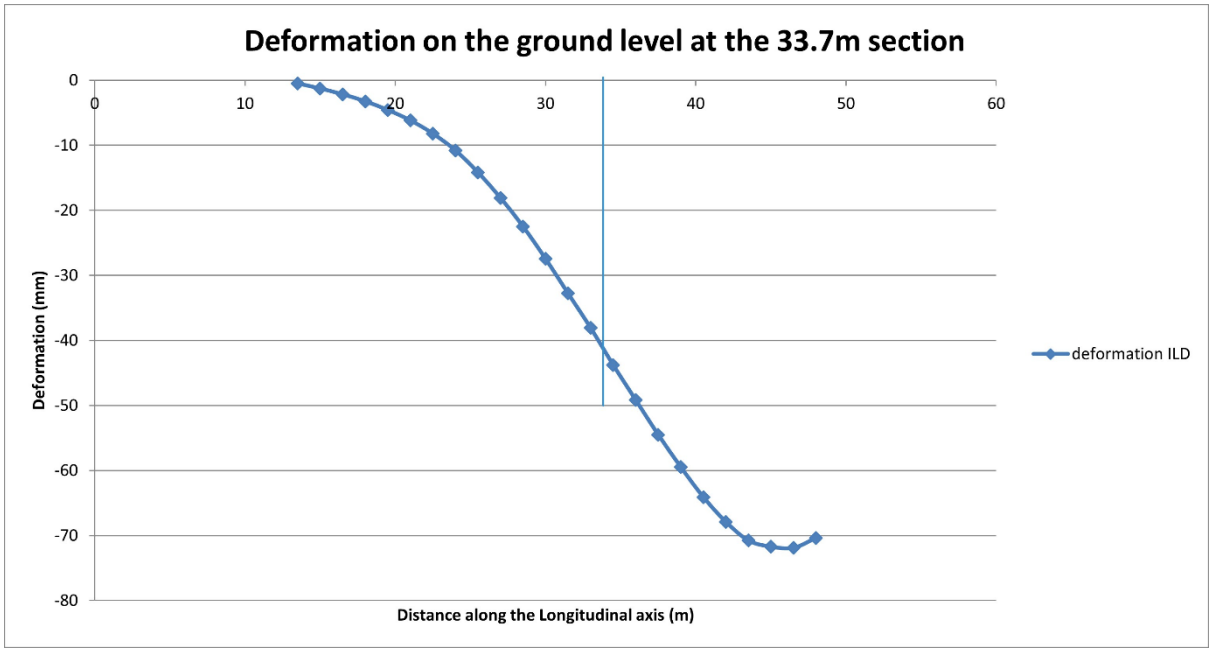

Fig. 4.7 Deformation ILD at 33.7 m section on the ground surface

The X-axis denotes the tunnel head position, henceforth, the first point starts with X-coordinated of 13.5 m. The vertical lines denote the point which are under the focusses. The deformations increase as we advance. The rate of deformation is seen to be less at the initial stages but it increased as the tunneling action advanced. Then the rate was seen to become a constant as long as the deformation reached a maximum value, after which the rate was seen to decrease and the sign of rate reversed. The deformation is then seen to happen in the opposite direction i.e., a bit of upheave is seen to happen as the tunnel advanced. The rebound becomes

predominant as the section under consideration shifts in the opposite direction of tunnel advancement. According to theoretical aspect, the deformation should have been constant after attaining a maximum value. Analysis was carried on a bit further, till phase 32, but significant changes were hard to notice. A reason could be due to stress re-distribution, but it wouldn't have given that predominant a rebound.

Another inference could be that, Mohr-Coulomb method designed the unloading curve as an elastic curve, same as the loading curve. Maybe, that is what gave the curve a line of symmetry. Some other modelling method like soft clay or creep model could have given results which were closer to the realistic ones. However, the loading simulation was done by this model was done with considerable amount of precision.

4.3 STRESS DISTRIBUTION

Tunneling involves a set of actions being done in a sequence. These actions have an outcome in the form of pressure exerted on the soil and overlying structures. Also, actions produce reactions. Hence the whole phenomenon is a complicated interplay of stress distribution and re-distribution. Various types of stresses can develop in the soil during tunneling. Plaxis 3D gives a simplified simulation of those stresses and its distributions. Those can be accessed from the *Stresses* option in the menu bar. Stresses can be of many types, cartesian meaning along the coordinates shown, principal stresses meaning along the principal directions. Again, each of these two can be effective or total stresses which can be used according to the drainage and the soil type. Here as we are dealing with long term behavior, we consider effective stresses.

4.3.1 *Variation of σ'_{xx} with depth*

The effective stress along X-direction, is plotted against the depth. The extent to which consideration is done is the top of the tunnel. Two different locations are taken separately along the Y-direction, viz., 25.3 m and 33.7 m. For each of those locations, Z v/s σ'_{xx} are plotted for all the phases. However, to avoid overcrowding of lines, two alternate phases are omitted. Fig. 4.8 and 4.9 show the plots for 33.7 m and 25.3 m respectively. Also, the sign convention here is reversed, i.e., the actual graphs were supposed to be in the third quadrant. To maintain the convention, the stress values have been considered as positive.

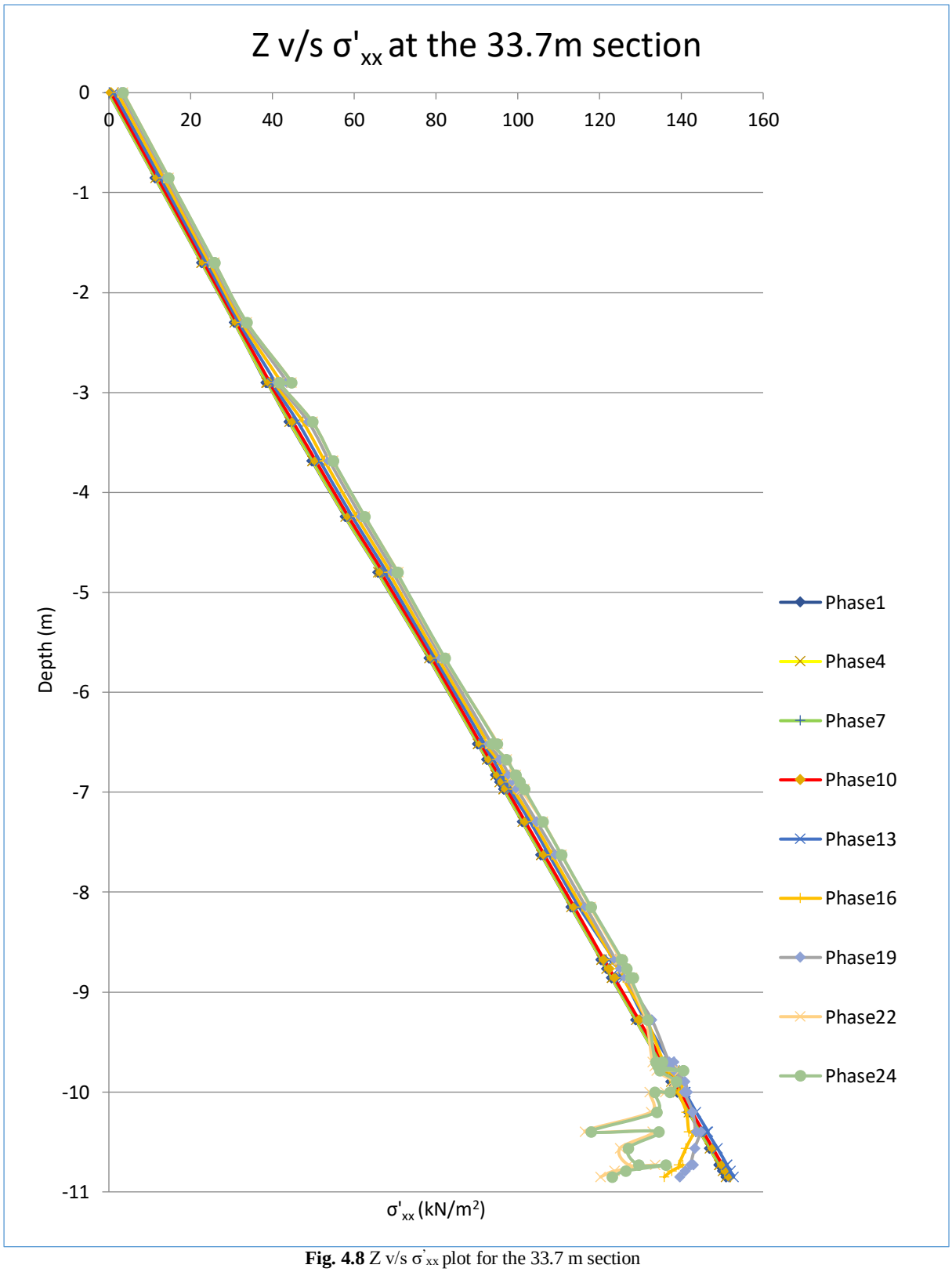

Fig. 4.8 Z v/s σ'_{xx} plot for the 33.7 m section

σ'_{xx} values are seen to increase, from a bare zero value, with depth for the initial phases. The phase where the tunnel crossed the said cross-section, anomaly started to be visible. From phase 16, the values started decreasing near the tunnel top. After that, irregular shaped lines are seen to be formed.

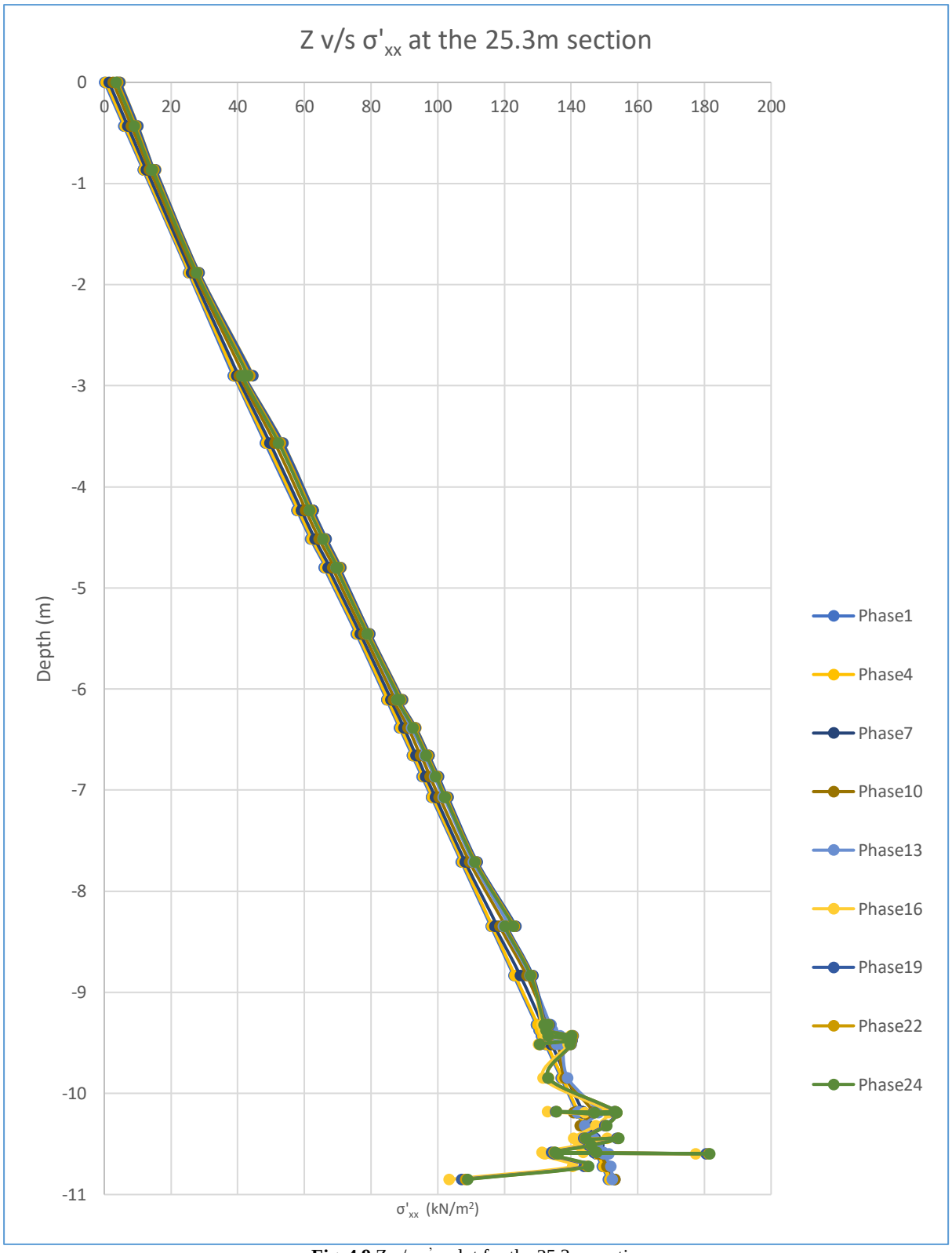

Fig. 4.9 Z v/s σ'_{xx} plot for the 25.3 m section

Similarly, for the 25.3 m section, the initial phases recorded an increase in the stress values near the tunnel top. But the graphs started becoming irregular and values decreased as the tunnel advanced further.

4.3.2 *Variation of σ'_{yy} with depth*

Fig. 4.10 and 4.11 show the variation of σ'_{yy} with depth for 33.7 m and 25.3 m sections respectively, with all the other parameters remaining same.

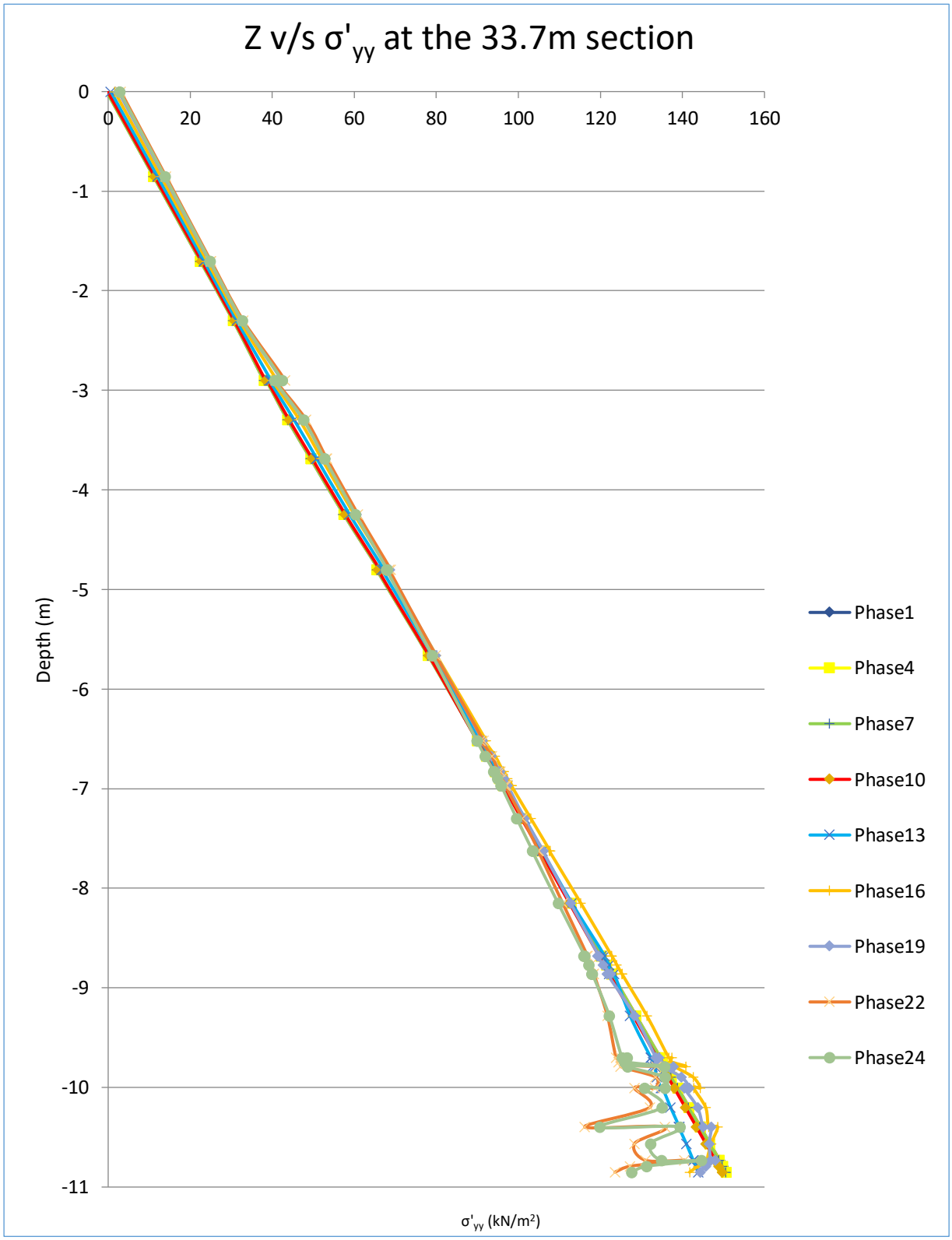

Fig. 4.10 Z v/s σ'_{yy} plot for the 33.7 m section

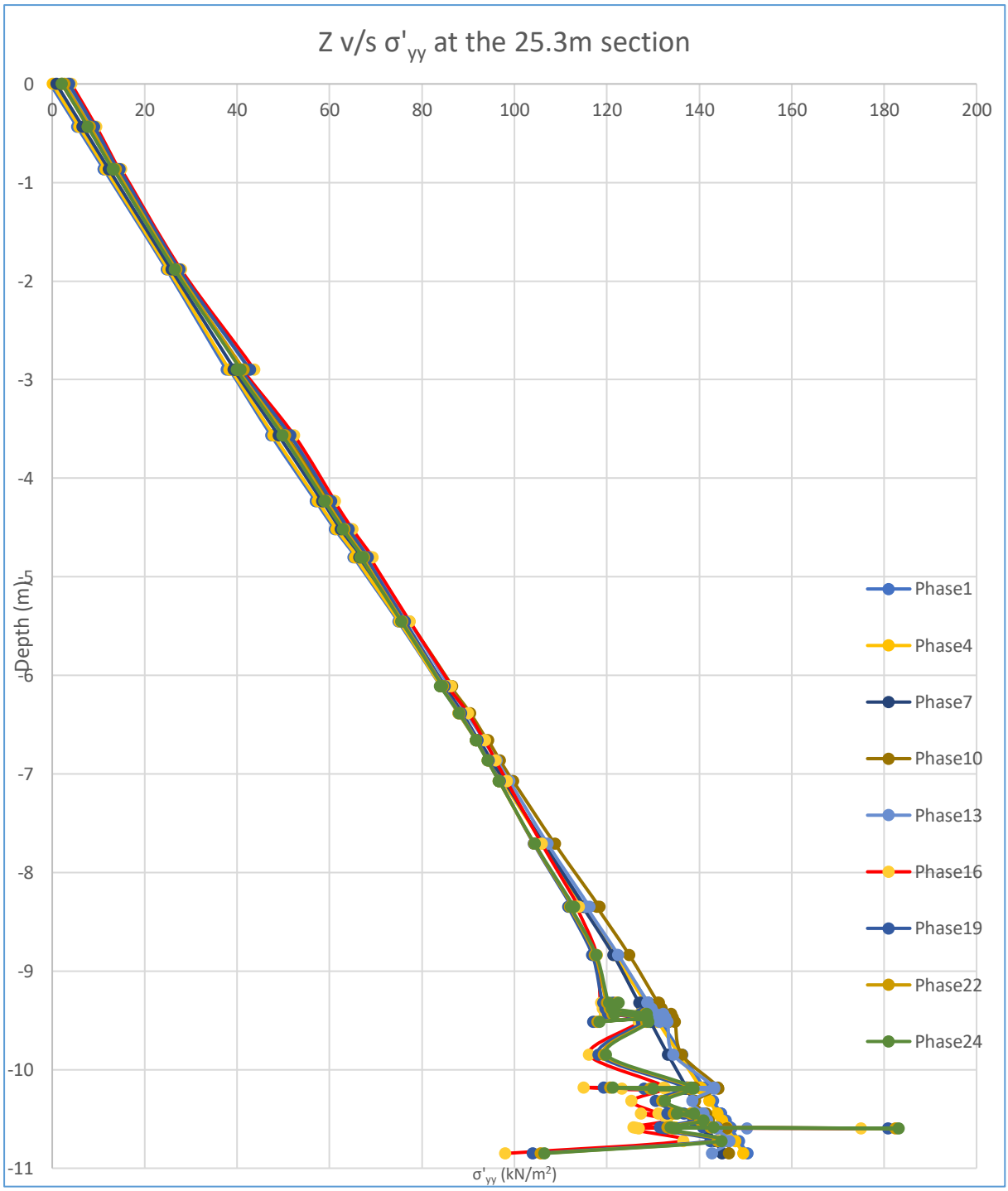

Fig. 4.11 Z v/s σ'$_{yy}$ plot for the 25.3 m section

Same as σ'$_{xx}$, variation if σ'$_{yy}$ with depth showed an increase with depth unanimously starting from an approximately zero value. In the initial phases, the lines continued, almost as linear lines. However, as the tunnel head crossed the section under consideration, the stress values started decreasing. Also, the lines patterns weren't seen to be uniform, rather kinks started getting visible near the top of the tunnel. The stresses were seen to decrease and then increase again, for the phases were downstream of the cross-section. But here also, the absolute values of the stresses were taken to keep up with the convention.

4.3.3 *Variation of σ'_{zz} with depth*

The most significant of the stresses, $\sigma'_{zz,}$ have been plotted against depth. Fig. 4.9 and 4.10 show the Z v/s σ'_{zz} variations for 33.7 m and 25.3 m respectively.

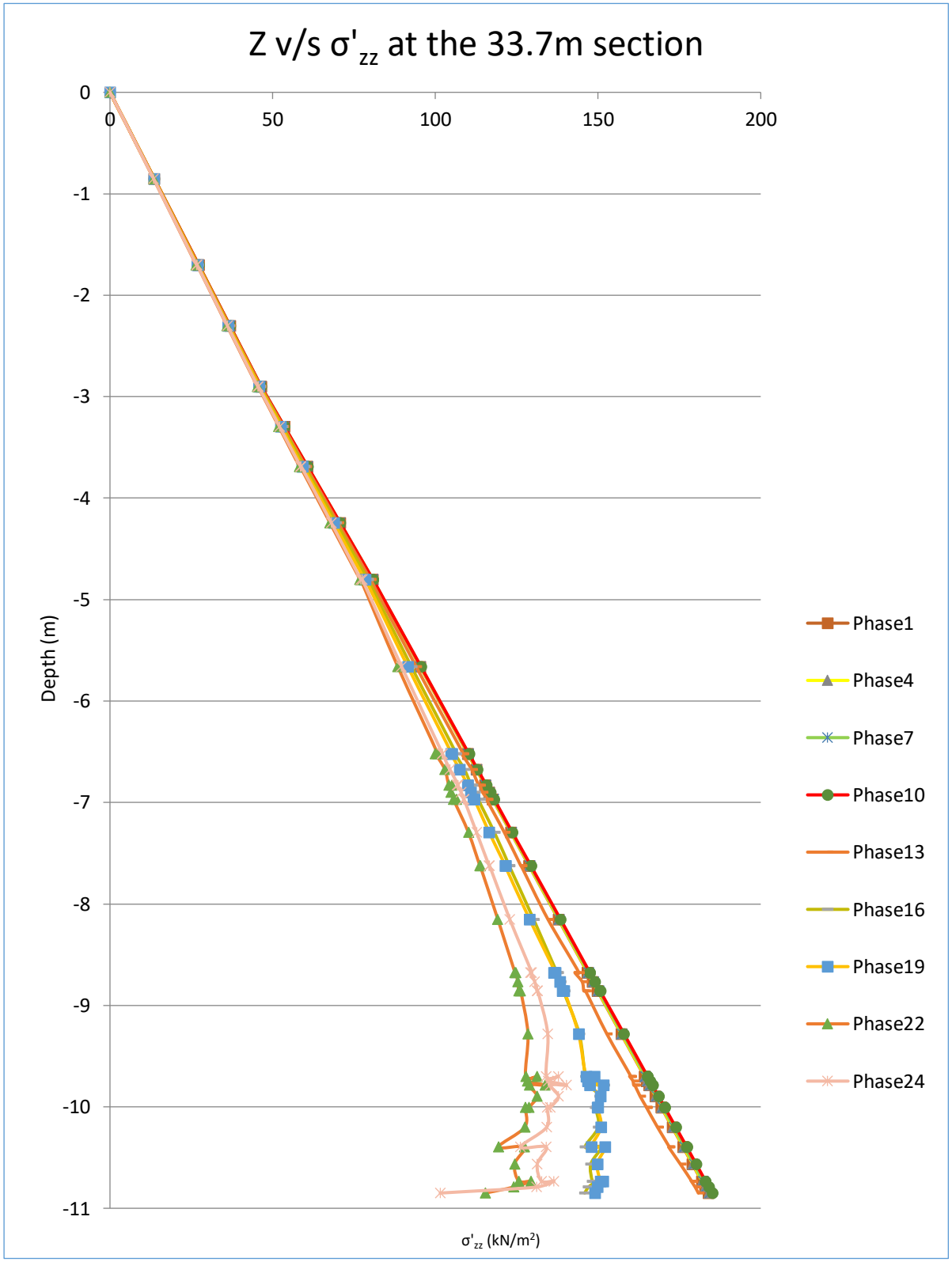

Fig. 4.12 Z v/s σ'_{zz} plot for the 33.7 m section

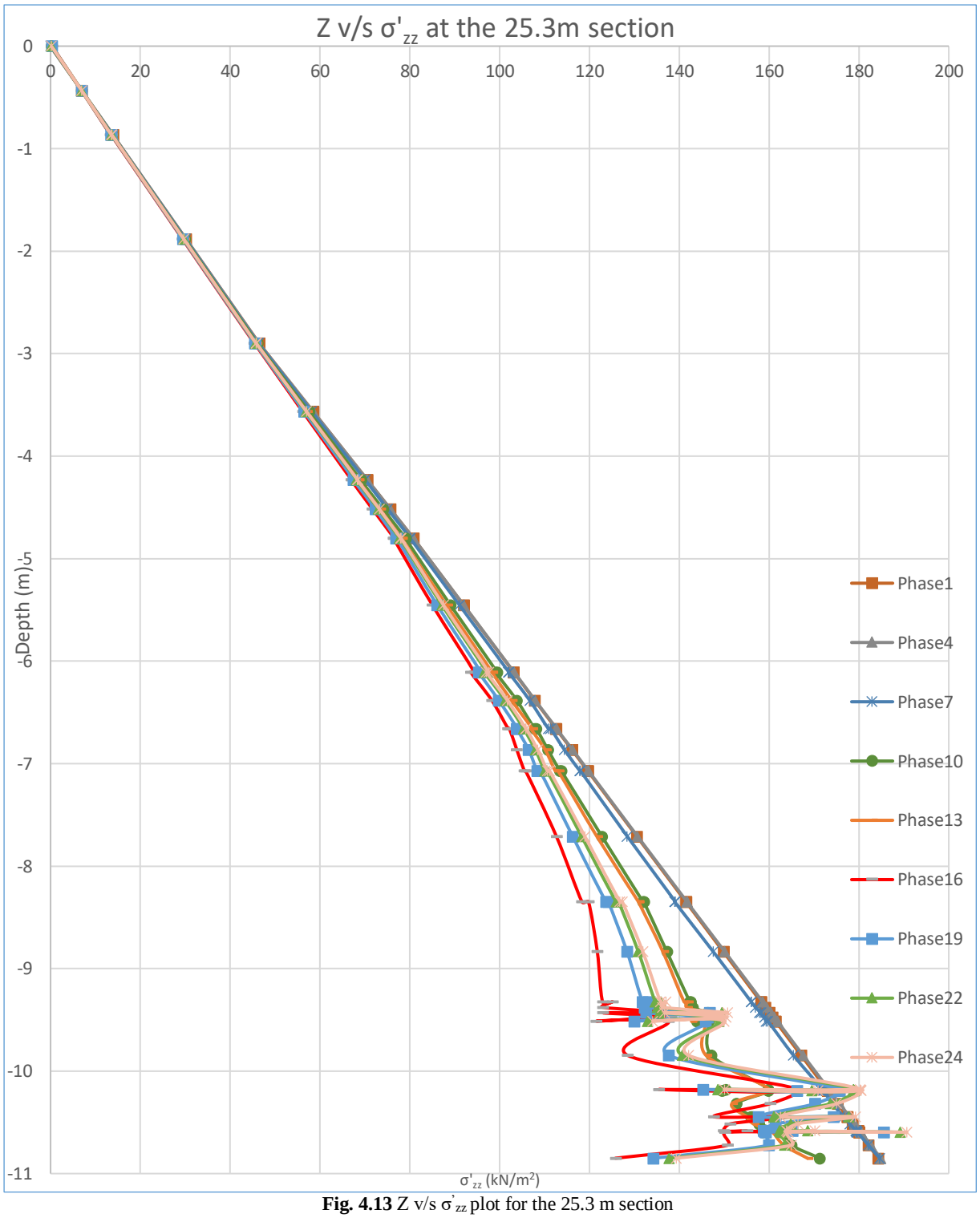

Fig. 4.13 Z v/s σ'_{zz} plot for the 25.3 m section

Similarly, for σ'_{zz}, the values start increasing from zero with depth till the tunnel top. The initial phases hardly showed any differences, with the lines overlapping on one another. As that particular phase came, where the tunnel head crossed the section taken, the lines started shifting towards the inner side and the uniformity of the lines was nullified. The stresses started increasing and decreasing in an irregular fashion. This goes down to the intricate way the tunnel behaves when it comes to the stress distribution and the soil behavior.

4.4 STRESS PATH

The study of shear strength of soil is predominantly being monitored by showing the Mohr's stress circle at different stages of loading/unloading. However, it becomes difficult to plot a number of circles. Also, it makes things confusing at the same time. In that case, a stress path might be used to show the changes in stress in the soil.

A stress path is therefore a curve or straight line or a combination of both, which is the locus of a series of stress points showing the changes in stress in a soil specimen in-situ, during loading. This is caused by forces of nature. This idea of depicting the maximum shear stress acting on the soil sample corresponding to its Mohr's circle was given by Lambe and Whitman (1969). The graph is basically a q v/s p graph, where,

$$p = \frac{\sigma 1+\sigma 3}{2} \tag{4.1}$$

$$q = \frac{\sigma 1-\sigma 3}{2} \tag{4.2}$$

Fig. 4.11 shows how stress path curve is generated from its corresponding Mohr's circle. σ_1 denotes the maximum principal stress and σ_3 denotes the minimum principal stress. For effective conditions, effective stress parameters are used (i.e., σ'_1, σ'_3). If the curve is heading towards right in the upward direction, it's a construction at the top. For an excavation, it will head towards left bottom. Similarly, it shows right-down and left-up direction for lateral confinement and expansion respectively.

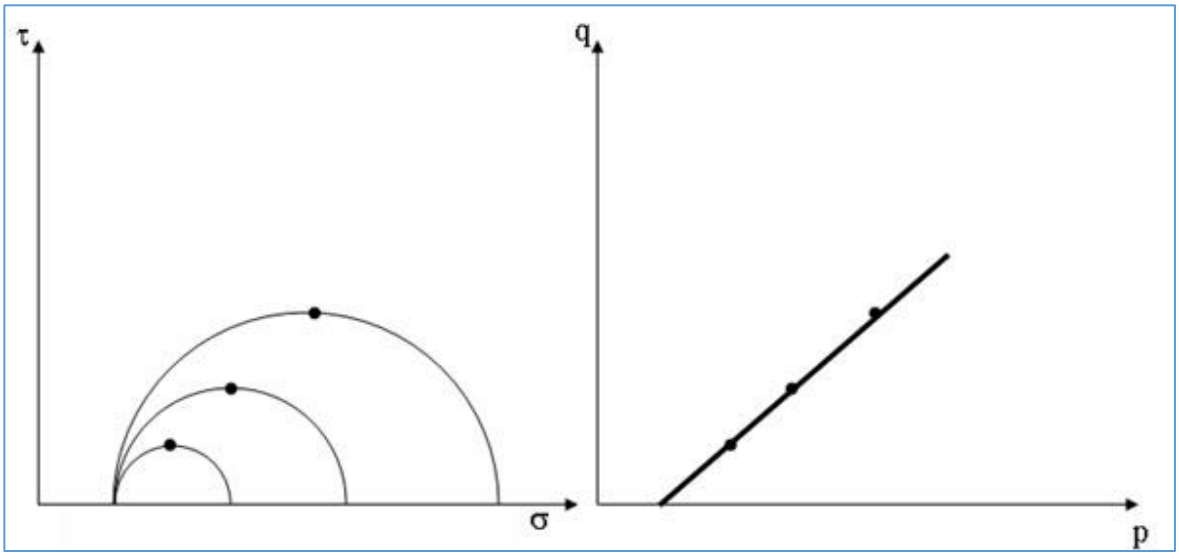

Fig. 4.14 (a) Mohr's circle **(b)** Respective Stress path

Stress paths are plotted for two different longitudinal distances (33.7 m, 25.3 m) and for four different depths in each case (tunnel top, 10.8 m, 8.86 m, 6.67 m).

4.4.1 *Stress path at 33.7 m section*

Effective parameters p' and q' are obtained from the *Stresses* option in the output window. At the 33.7 m section, values of these effective parameters are noted for all the phases of the tunnel advancement. And this is done for four different depths as mentioned earlier. The graph looks as shown in Fig. 4.15.

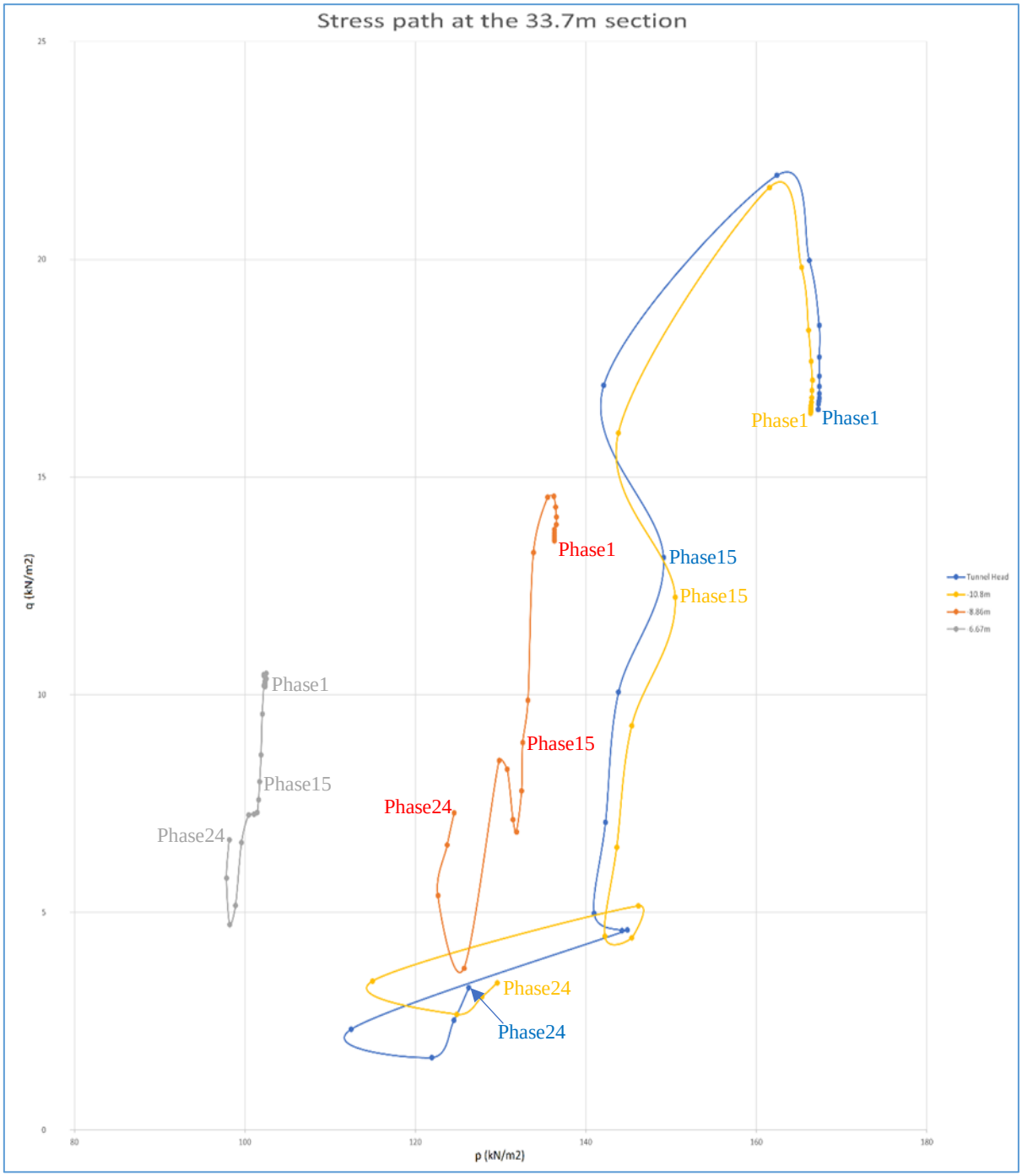

Fig. 4.15 Stress path for the 33.7 m section

The Mohr's circles for all the phases and depths are also drawn, in order to analyze things better. Fig. 4.16 (a), (b) and (c) show the circles for depths 10.8 m, 8.86 m and 6.67 m respectively. The tunnel top is seen to be very near to the 10.8 m level, hence has been left out.

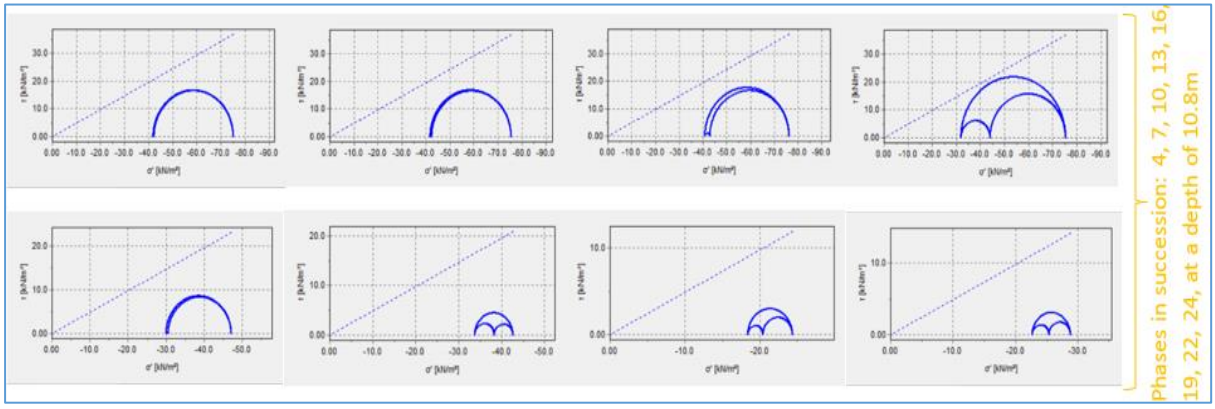

Fig. 4.16 (a) Mohr's circle at 10.8 m depth for the phases mentioned

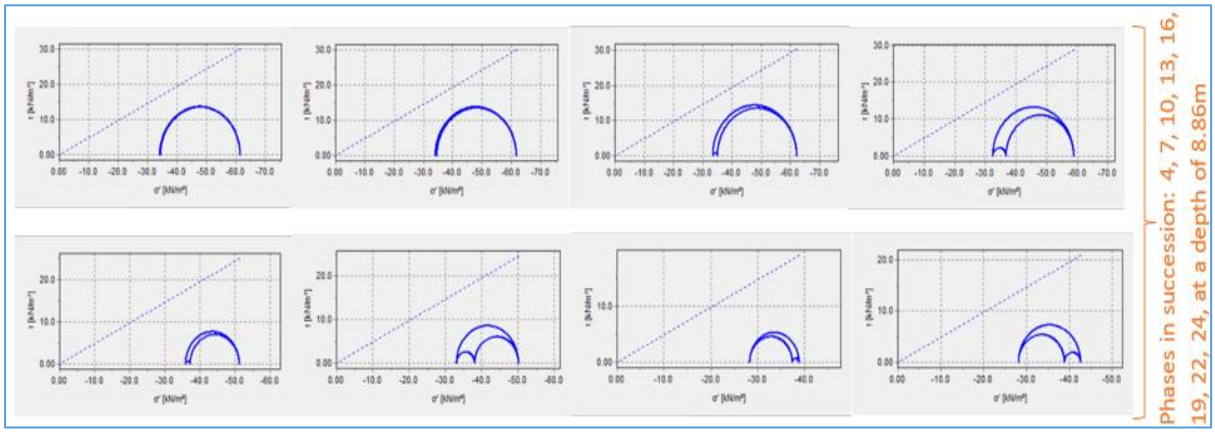

Fig. 4.16 (b) Mohr's circle at 8.86 m depth for the phases mentioned

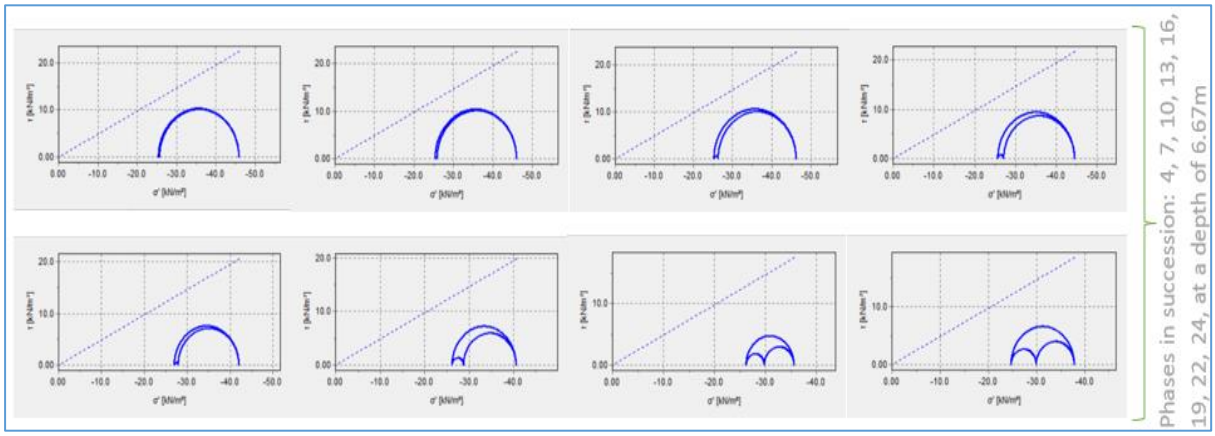

Fig. 4.16 (c) Mohr's circle at 6.67 m depth for the phases mentioned

Further explanations about the stress path and Mohr's circles generated will be done under the next sub-heading. Different colors have been used to depict the different depths under consideration.

4.4.2 *Stress path at 25.3 m section*

Similarly, the effective parameters are extracted from the *Stresses* feature within the output window. These parameters are recorded for each stage of tunnel advancement at the 25.3 m section, and this process is repeated at four distinct depths, as previously specified. The resulting graph is illustrated in Figure 4.17.

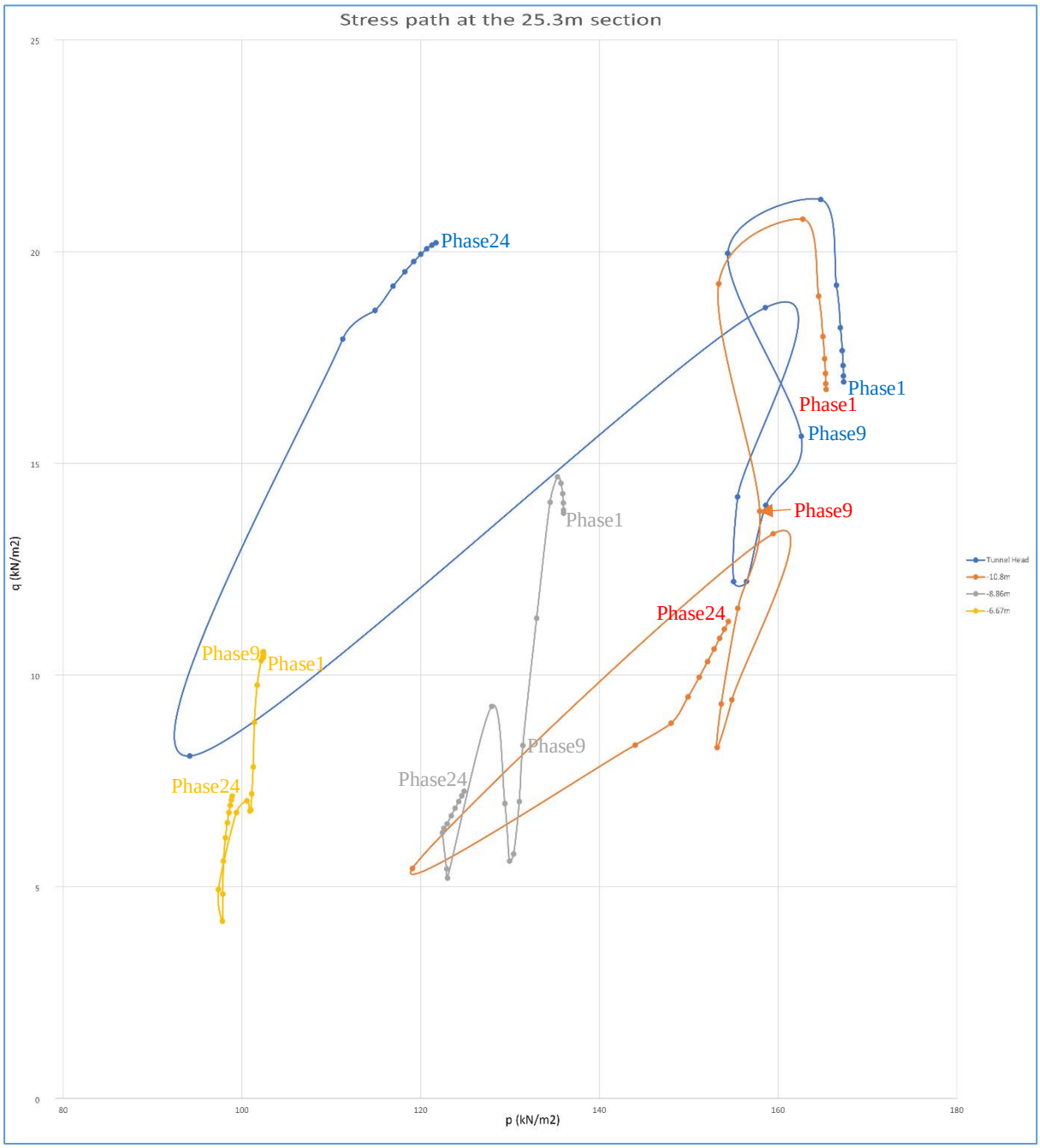

Fig. 4.17 Stress path for the 25.3 m section

The color combinations are very significant, as they denote the different depths at which the study is being done. Stress paths at close to each other are seen to differ by a small distance only. But with significant change in depth, stress paths change vividly. Irrespective of the section and the depth considered, the initial stages show an increase in the 'q' value but the 'p' value doesn't change. This means the major principal stress increase and the minor principal stress decrease by the same amount.

The next phase of the graph shows a decline. This happens after the tunnel has advances by some amount. The patten then changes as the tunnel crosses the particular section under consideration. The 3-D Mohr's circle diameter and position changes accordingly. The tunnel phases where the tunnel crosses the said cross-section is mentioned in the figures, apart from the initial and the final phases.

The tunneling operation is complex and is a combination of events happening simultaneously. Henceforth, we get to see the graph heading towards the various directions. A clear explanation for all those graph movements is hard to get by, and therefore take it as it is. A detailed study is need to understand each and every step of the stress paths and relate it to the respective Mohr's circles.

4.5 STUDY OF VOLUME LOSS

Any tunneling action, no matter how stiff or dense the soil is, involves some degree of ground loss. The loss of ground may be defined as volume of material that had been excavated out in excess of the theoretical volume within the outer diameter of the final tunnel lining. Typically, the loss of volume (V_L) is given by the equation,

$$V_L = \frac{\Delta V}{V_0} \times 100\ \% \tag{4.3}$$

Where, 'ΔV' denotes the ground loss,

'V_0' denotes the volume enclosed by the final tunnel lining.

Traditionally, V_L assumes values from different equations, depending on the elasticity of the soil and other parameters. However, in this study we have calculated the volumes manually, with the help of AutoCAD 2007 software. Also, 'ΔV' can be calculated using the formula given in eq. 4.4.

$$\Delta V = 2.5 i S_{max} \tag{4.4}$$

Where, 'i' denotes the distance of point of inflexion,

'S_{max}' denotes the maximum settlement i.e., along the center-line.

Again, the value of 'i' can be obtained from the formula,

$$\frac{i}{a} = \left(\frac{z}{2a}\right)^{0.8} \tag{4.5}$$

Where, 'z' denotes the depth of the tunnel center below the ground level,

'a' denotes the radius of the tunnel.

Another significant equation in this context is given as eq. 4.6. This can be used to check the settlements obtained at various points of the inverted bell curve.

$$S = S_{max}\, e^{\left(-\frac{x^2}{2i^2}\right)} \tag{4.6}$$

The volume loss percentage, from previous study, bears a range, within which the tunnel is said to be stable. If the value of V_L lies in the limit of 4-6%, stability of the tunnel is said to be there. Here the study is done at the 33.7 m section, for a phase where the tunnel has already surpassed the section, viz., phase 19. The ordinates of the ground deformation, for phase 19 at that particular section is already obtained. The deformation profile is given in the Fig. 4.18.

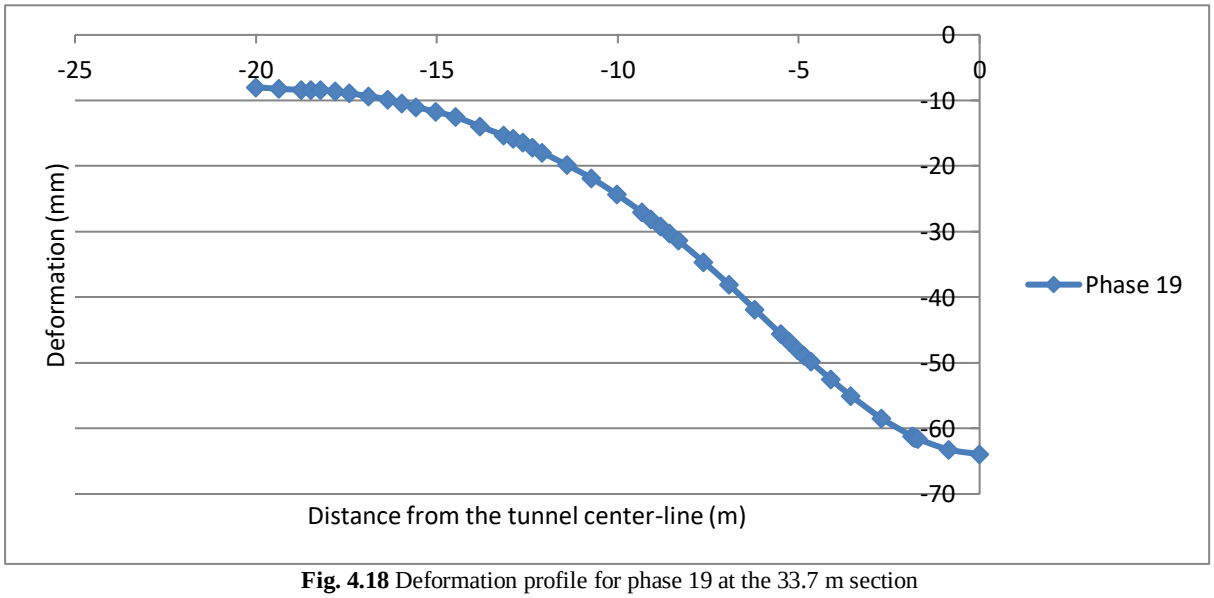

Fig. 4.18 Deformation profile for phase 19 at the 33.7 m section

The ordinates are then plotted in AutoCAD 2007, and the *Area* option gives us the area of the space in-between those points. Fig. 4.19 shows the AutoCAD window, where the area was calculated. The area thus obtained was seen to be 0.6044 m^2. It is noteworthy that here all the volumes calculated are in the forms of areas i.e., by taking unit length.

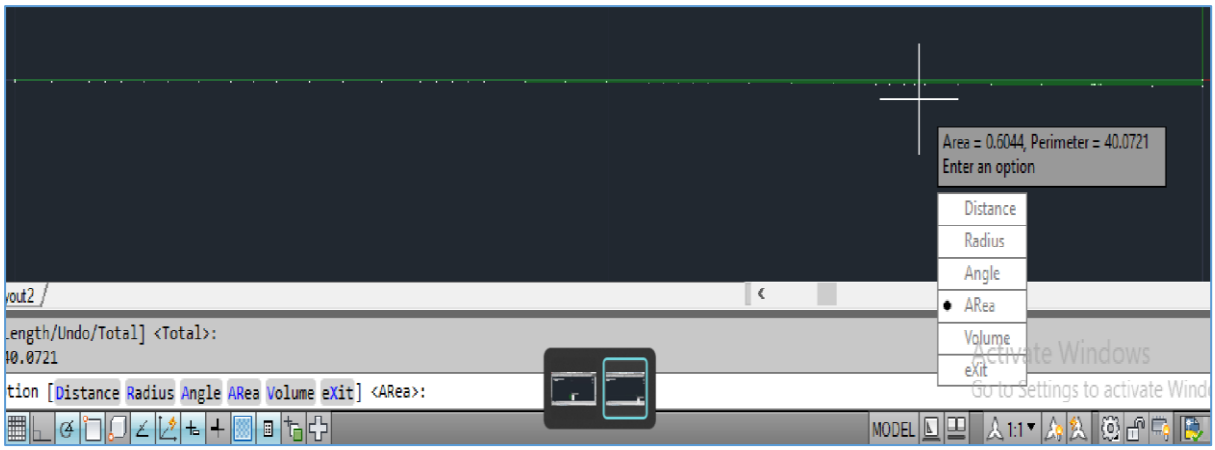

Fig. 4.19 AutoCAD window showing the area calculation

Then comes the next task, that is finding the area under the final tunnel lining. For this, we need to know the co-ordinates of the tunnel lining that was there initially. Then, nodes corresponding to those points were chosen and displacements of all those points were noted. Only the displacements along the X and Z directions were what was needed. Sometimes the exact nodes were not found. In those cases, the nearest node values were taken. Then the displacement values were added to the initial co-ordinates and we ended up the final lining co-ordinates. This change in value was seen due to the soil surcharge present and the other stresses that were activated by the process of tunneling. After that, the same procedure was conducted using AutoCAD, to get the area. Fig. 4.20 shows the AutoCAD window with the final lining

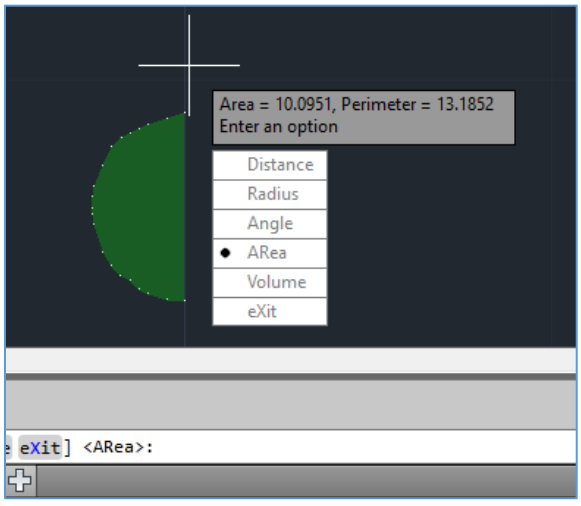

Fig. 4.20 The final tunnel lining and its area

shown and the area calculated. The final area under the area depicted was found to be 10.0951 m^2.

Hence, we get the values of ΔV and V_0 as 0.6044 m^2 and 10.0951 m^2 respectively. Therefore, the volume loss as calculated using eq. 4.3 is obtained as 5.9871%. This value well lies in the range as mentioned earlier. Hence the stability of the tunnel-ground system can be said to be intact.

Chapter 5 : **CONCLUSION, LIMITATION AND FUTURE SCOPE OF STUDY**

This study seeks to offer an overview of the research conducted utilizing finite element analysis within the PLAXIS 3D software. The study involved creating a 3D structural model of the problem geometry in PLAXIS, followed by a series of analyses to understand the complex interactions between the tunnel and the surrounding soil. Furthermore, it serves as a valuable resource for designers looking to simulate real-world scenarios in their field. The study provides the following key takeaways.

5.1 CONCLUSION

The following conclusion can be drawn from the present study:

1. Tunneling in soil involves many actions being performed in sequence. Firstly, a certain distance inside the soil is cut out manually and the TBM is assembled and placed inside the conduit formed. The tunnel head then cuts the soil and sweeps out the plastic debris. Tunnel face pressure in the longitudinal direction is provided for stability of the soil at the head location, whereas, the grout pressure in the radial direction, gives stability to the unlined portion of the soil. The TBM also lines the tunnel and gives a jacking thrust in order to move in the forward direction.
2. PLAXIS 3D gives a simulation of the field conditions and provides the designers with appropriate guidance while carrying out tunneling actions.
3. At a particular cross-section, the deformation curve of the ground surface resembles an inverted bell shape (i.e., an inverted Gaussian curve). At the initial phases, the deformation curves were closed to one another. With the tunnel advancement, the gaps between them increased and assumed a maximum value at phases when the section was crossed. Then again, the gaps decreased, sometimes overlaps were also visible. A bit of soil rebound was also present.
4. If we go along the longitudinal direction, the ground surface deformation showed a particular pattern for all the phases. The maximum deformations were seen to come at those locations where the tunnel is unlined, or where the grout pressure acts. Moreover, some rebound was also recorded after the tunnel had reached a particular distance.

5. The deformation of a particular point on the ground surface, with tunnel advancement, was seen to increase, reach a maximum value and then decrease, even though, theoretically, it should become constant at some point of time. Hence, some soil heaving was seen in this case also.
6. The soil rebound or heaving was seen in almost all types of deformation patterns. A part of it is attributed to the stress re-distribution. However, another reason could be that, the Mohr-Coulomb model considers the unloading curve as an elastic profile.
7. Stress variation with depth for all the directions, showed a pattern. It increased with depth for a particular phase, and across the phases it remained approximately constant, till that phase where the tunnel head crossed the cross-section. From that point onwards, the curve started drifting towards the lesser values and the uniformity of the lines got disrupted. Moreover, kinks were visible in those curves.
8. A general study on the various terms related to the tunnel is seen, and their inter-relationship is highlighted. Percentage volume loss of ground on tunneling action is done, for a particular location. And that value is seen to be well within the range, and henceforth, the tunnel could be said to be in a stable condition.

5.2 LIMITATIONS

This study has a restricted focus, and the subsequent are a few of its drawbacks:

1) This a numerical study only. Physical data is absent.
2) Numerical analysis can never give the exact simulation of things happening in the field. It can merely act as a guideline.
3) PLAXIS 3D doesn’t give us the opportunity to chose the number of nodes or elements it creates. Hence, getting the desired node of element, at times, becomes difficult.
4) The model considered (Mohr-Coulomb) haven’t designed the unloading curves as expected.
5) Time factor is not considered during the model is prepared.
6) Arching action in soil isn’t considered.

5.3 FUTURE SCOPE OF STUDY

Further research has the potential to address the study's limitations, with the following areas being worthy of consideration:

1) Developing a physical model to validate the numerical data.

2) Centrifuge testing with the same soil and tunnel parameters could be performed at a particular acceleration, to match the numerical deformation results.
3) Deploying a finer mesh generation to get to the exact node location, with greater probability and conviction.
4) Adoption of a different soil model type like *Soft Soil* model to get to better results.
5) Adoption of *Soft Soil Creep* model to incorporate the time effects in the tunneling process.

REFERENCE

Attewell, P. B., Yeates, J., and Alan Selby, R., *Soil Movements Induced by Tunnelling and Their Effects on Pipelines and Structures*, Blackie, London, UK, 1986.

Peck, R. B., 1969, *Deep excavation and tunneling in soft ground*. In *Proc., 7th Int. Conf. on Soil Mechanics and Foundation Engineering*. London: International Society of Soil Mechanics and Foundation Engineering.

Kimura, T., 1981. Centrifugal testing of model tunnels in soft clay. *Proc. 10th ICSMFE, 1981*, *1*, pp.319-322.

Mair, R.J., 1979. Centrifugal testing of model tunnels in soft clay. *Ph. D thesis, Cambridge University*.

Ng, R.M., 1984. Ground reaction and behaviour of tunnels in soft clays.

Loganathan, N. and Poulos, H.G., 1998. Analytical prediction for tunneling-induced ground movements in clays. *Journal of Geotechnical and geoenvironmental engineering*, *124*(9), pp.846-856.

Lee, C.J., Wu, B.R., Chen, H.T. and Chiang, K.H., 2006. Tunnel stability and arching effects during tunneling in soft clayey soil. *Tunnelling and Underground Space Technology*, *21*(2), pp.119-132.

Greenwood, J.D., 2003. *Three-dimensional analysis of surface settlement in soft ground tunneling* (Doctoral dissertation, Massachusetts Institute of Technology).

Mattar, J., 2007. An investigation of tunnel-soil-pile interaction in cohesive soils.

Fattah, M.Y., Shlash, K.T. and Salim, N.M., 2013. Prediction of settlement trough induced by tunneling in cohesive ground. *Acta Geotechnica*, *8*, pp.167-179.

Fattah, M.Y., Shlash, K.T. and Salim, N.M., 2011. Settlement trough due to tunneling in cohesive ground. *Indian Geotech. J*, *41*(2), pp.64-75.

Likitlersuang, S., Surarak, C., Suwansawat, S., Wanatowski, D., Oh, E. and Balasubramaniam, A., 2014. Simplified finite-element modelling for tunnelling-induced settlements. *Geotechnical Research*, *1*(4), pp.133-152.

Soranzo, E., Tamagnini, R. and Wu, W., 2015. Face stability of shallow tunnels in partially saturated soil: centrifuge testing and numerical analysis. *Géotechnique*, *65*(6), pp.454-467.

Shabna, P.S. and Sankar, N., 2016. Numerical analysis of shallow tunnels in soft ground using Plaxis2D. *Int J Sci Eng Res*, *7*(4), p.978.

Soga, K., Laver, R.G. and Li, Z., 2017. Long-term tunnel behaviour and ground movements after tunnelling in clayey soils. *Underground Space*, *2*(3), pp.149-167.

Liu, K., Ding, W., Zhang, Q., Shi, P. and Yan, C., 2019. Stability analysis of earth pressure balance shield tunnel face considering soil arching. *Proceedings of the Institution of Civil Engineers-Geotechnical Engineering*, *172*(4), pp.377-389.

Shinde, N.T., Kuwar, S.R., Khairnar, A.P., Khairnar, Y.J. and Shivde, S.R., 2019. Tunnel Analysis using Plaxis 2D. *Int. J. Res. Eng. Sci. Man.*, *2*, pp.4-5.

Shinde, N.T., Kuwar, S.R., Khairnar, A.P., Khairnar, Y.J. and Shivde, S.R., 2019. Tunnel Analysis using Plaxis 2D. *Int. J. Res. Eng. Sci. Man.*, *2*, pp.4-5.

Alagha, A.S. and Chapman, D.N., 2019. Numerical modelling of tunnel face stability in homogeneous and layered soft ground. *Tunnelling and Underground Space Technology*, *94*, p.103096.

Kanagaraju, R. and Krishnamurthy, P., 2020. Influence of tunneling in cohesionless soil for different tunnel geometry and volume loss under greenfield condition. *Advances in Civil Engineering*, *2020*, pp.1-11.

Meng, F.Y., Chen, R.P., Liu, S.L. and Wu, H.N., 2021. Centrifuge modeling of ground and tunnel responses to nearby excavation in soft clay. *Journal of Geotechnical and Geoenvironmental Engineering*, *147*(3), p.04020178.

Qi, H., Cui, W., Li, H., Cheng, J., Kong, L., Wang, X., Zhang, J., Yang, G., Yue, H. and Song, X., 2021. Undrained Stability Analysis of Shallow Tunnel and Sinkhole in Soft Clay: The Cavity Contraction Method. *Applied Sciences*, *11*(19), p.9059.

Maji, V.B. and Adugna, A., 2016. Numerical modeling of tunneling induced ground deformation and its control. *International Journal of Mining and Geo-Engineering*, *50*(2), pp.183-188.

Ahmed, K.S., Sharmin, J. and Ansary, M.A., 2023. Numerical investigation of tunneling induced surface movement: A case study of MRT Line 1, Dhaka. *Underground Space*.

Boudjellal, D.E., Hafsaoui, A. and Korichi, T., 2018. Numerical Modeling by Plaxis Software (3D), the Effect of Digging a Tunnel on the Behavior of the Ground and Overlying Structures: Case: Subway of Algiers (Algeria). In *Engineering Challenges for Sustainable Underground Use: Proceedings of the 1st GeoMEast International Congress and Exhibition, Egypt 2017 on Sustainable Civil Infrastructures 1* (pp. 173-206). Springer International Publishing.

Sharmin, J., 2022. Numerical investigation of new austrian tunneling method and tunnel boring method for tunnel construction.

El-Nahhas, F.M., El-Mossallamy, Y.M. and El-Shamy, A.A., 2015. 3D analysis of ground settlement induced by mechanized tunnelling. In *14th International Conference on Structural and Geotechnical Engineering*.

EL HOUARI, N., 3D simulation of tunnel excavation in soft soil. *Journal of Science, Technology and Engineering Research*, *4*(1), pp.67-77.

Elarabi, H. and Mustafa, A., 2014. Comparison of numerical and analytical methods of analysis of tunnels. *Geotechnical aspects of underground construction in soft ground (August 4, 2014)*, pp.225-231.